Toxicology 464 (2021) 153028

Contents lists available at ScienceDirect

Toxicology

journal homepage: www.elsevier.com/locate/toxicol

Perfluorooctane sulfonate (PFOS) exposure of bovine oocytes affects early embryonic development at human-relevant levels in an *in vitro* model

Ida Hallberg [a,*], Sara Persson [a], Matts Olovsson [b], Marc-André Sirard [c], Pauliina Damdimopoulou [d], Joëlle Rüegg [e], Ylva C.B. Sjunnesson [a]

[a] Department of Clinical Sciences, Division of Reproduction, The Centre for Reproductive Biology in Uppsala, Swedish University of Agricultural Sciences, SE-750 07, Uppsala, Sweden
[b] Department of Women's and Children's Health, Uppsala University, SE-751 85, Uppsala, Sweden
[c] Department of Animal Sciences, Laval University, QC G1V 0A6, Quebec, Canada
[d] Division of Obstetrics and Gynaecology, Department of Clinical Science, Intervention and Technology, Karolinska Institutet and Karolinska University Hospital, SE-141 86, Stockholm, Sweden
[e] Department of Organismal Biology, Program of Environmental Toxicology, Uppsala University, SE-752 36, Uppsala, Sweden

ARTICLE INFO

Handling Editor: Mathieu Vinken

Keywords:
Perfluorooctane sulfonate
Bovine *in vitro* embryo production
Oocyte maturation
Lipid distribution
Gene-expression

ABSTRACT

Perfluorooctane sulfonate (PFOS) has been added to Stockholm Convention for global phase out, but will continue to contribute to the chemical burden in humans for a long time to come due to extreme persistence in the environment. In the body, PFOS is transferred into to the ovarian follicular fluid that surrounds the maturing oocyte. In the present study, bovine cumulus oocyte complexes were exposed to PFOS during 22 h *in vitro* maturation. Concentrations of 2 ng g^{-1} (PFOS-02) representing average human exposure and 53 ng g^{-1} (PFOS-53) relevant to highly exposed groups were used. After exposure, developmental competence was recorded until day 8 after fertilisation. Blastocysts were fixed and either stained to evaluate blastomere number and lipid distribution using confocal microscopy or frozen and pooled for microarray-based gene expression and DNA methylation analyses.

PFOS-53 delayed the first cleavage to two-cell stage and beyond at 44 h after fertilisation ($p < .01$). No reduction of proportion blastocysts were seen at day 8 in either of the groups, but PFOS-53 exposure resulted in delayed development into more advanced stages of blastocysts seen as both reduced developmental stage ($p = .001$) and reduced number of blastomeres ($p = .04$). Blastocysts showed an altered lipid distribution that was more pronounced after exposure to PFOS-53 (increased total lipid volume, p=.0003, lipid volume/cell $p < .0001$) than PFOS-02, where only decreased average lipid droplet size (p=.02) was observed. Gene expression analyses revealed pathways differently regulated in the PFOS-treated groups compared to the controls, which were related to cell death and survival through *e.g., P38 mitogen-activated protein kinases* and *signal transducer and activator of transcription 3,* which in turn activates *tumour protein 53 (TP53)*. Transcriptomic changes were also associated with metabolic stress response, differentiation and proliferation, which could help to explain the phenotypic changes seen in the blastocysts. The gene expression changes were more pronounced after exposure to PFOS-53 compared to PFOS-02. DNA-methylation changes were associated with similar biological functions as the transcriptomic data, with the most significantly associated pathway being *TP53.* Collectively, these results reveal that brief PFOS exposure during oocyte maturation alters the early embryo development at concentrations relevant to humans. This study adds to the evidence that PFOS has the potential to affect female fertility.

1. Introduction

Per- and polyfluoroalkyl substances (PFASs) are a large group of man-made chemicals used in a range of industrial applications and consumer products (Gluge et al., 2020). Due to their wide use and persistent nature, PFASs are found worldwide, exposing humans through food, drinking water, inhalation of dust and dermal contact (DeLuca et al., 2021; Poothong et al., 2020). During the last 60 years,

* Corresponding author.
E-mail address: ida.hallberg@slu.se (I. Hallberg).

https://doi.org/10.1016/j.tox.2021.153028
Received 1 September 2021; Received in revised form 20 October 2021; Accepted 4 November 2021
Available online 8 November 2021

perfluorooctane sulfonate (PFOS) and perfluorooctanoic acid (PFOA) have been the most widely used PFASs. Since potential health effects have been associated with exposure, phase-out of production and distribution of PFOS was initiated in the beginning of 21 st century and PFOS was included in Annex B of the Stockholm Convention of Persistent Organic Pollutants in 2009 (UNEP, 2009). This led to substitution with other PFASs in production. In general, phase-out of PFOS seems to result in decreased human serum levels (Bjerregaard-Olesen et al., 2016; Calafat et al., 2007; Glynn et al., 2012). Yet, due to their long half-life (Li et al., 2018; Zhang et al., 2013), it is inevitable that the exposure will persist for decades to come. PFOS is still the most detected PFAS in environmental and biological samples and present in serum in humans worldwide (Kannan et al., 2004). The average PFOS serum concentration measured in humans ranges from 4−20 ng mL^{-1} (Bjerregaard-Olesen et al., 2016; Calafat et al., 2007; Kim et al., 2020). Occupational exposure, as well as local contamination of drinking water can widely exceed the exposure of the general population (Li et al., 2018), and fire fighters with occupational exposure have significantly higher concentrations compared to controls (Rotander et al., 2015).

PFOS has been associated with reduced birth weight and poorer immunisation in response to vaccines in children, and to higher serum cholesterol in adults (Steenland et al., 2009). Furthermore, PFASs cross the ovarian blood-follicle barrier and have been found in ovarian follicular fluid in similar concentrations as in serum (Heffernan et al., 2018; Kang et al., 2020; McCoy et al., 2017; Petro et al., 2014). It also passes the placenta, exposing the foetus *in utero* (Mamsen et al., 2019) and is further secreted in milk, exposing the nursing infant (Kärrman et al., 2007). The evidence for adverse health effects related to reproductive outcomes in humans has been found to be insufficient to draw anyconclusions (Schrenk et al., 2020).

The process of forming a healthy offspring starts with the germ cell. In the female, the developmental competence of the oocyte is dependent on the folliculogenesis where the environment surrounding the oocyte consists of, for example, growth factors and sex steroids stimulating oocyte development. The final stage of oocyte maturation (from late antral stage) is an especially sensitive period where many critical events take place. At this point, the oocyte will resume the first meiosis and final nuclear and cytoplasmic maturation will occur in parallel with preparation for the genetic program that will drive early embryo development. Oocyte characteristics, as well as timing of events during early embryo development, are significantly different between species (Ménézo and Hérubel, 2002). The bovine oocyte maturation and early embryo development share many features with human oocyte maturation and early pre-implantation embryo development, making the bovine *in vitro* model an attractive alternative to rodent studies for toxicological and reproductive studies (Alm et al., 1998; Grossman et al., 2012; Hallberg et al., 2019; Jorssen et al., 2015; Krogenaes et al., 1998; Ménézo and Hérubel, 2002; Santos et al., 2014). The *in vitro* embryo production (IVP) set-up enables the study of specific windows, including the final 22 h of oocyte maturation (*in vitro* maturation, IVM) and the consequence for the subsequent early embryo development. IVP allows for phenotypic studies of the pre-implantation embryo to detect alterations during development using morphological assessments (IETS, 2010), including staining for further phenotypic characterisations (Gonzalez and Sjunnesson, 2013; Hallberg et al., 2019; Laskowski et al., 2017). Furthermore, microarray platforms, and more recently RNA sequencing techniques, have been developed to study the early embryo transcriptome (Robert et al., 2011) and methylome profiles (Saadi et al., 2014), which further contributes to the understanding of embryo interaction with their microenvironment, with the benefit of studying pathways rather than individual genes.

Even though PFOS has been manufactured for more than 60 years, information about potential toxicity to the female gamete and the consequences for female fertility is scarce. This is especially true for concentrations relevant to humans. However, PFOS has been associated with outcomes related to ovarian function, as recently reviewed (Ding et al., 2020). Human cohorts have shown associations with PFOS and longer time to pregnancy and effects on the menstrual cycle (Fei et al., 2009; Lopez-Espinosa et al., 2011; Whitworth et al., 2012; Zhou et al., 2017), which is supported by experimental animal studies (Dominguez et al., 2016; Feng et al., 2015). Therefore, the aim of this study was to investigate whether and how PFOS exposure during final oocyte maturation affects the pre-implantation embryo development. Concentrations of PFOS were based on levels previously reported in human ovarian follicular fluid, and the bovine IVP model was used to study its impact on the morphological and phenotypic characteristics of the embryos as well as on gene expression and epigenetic patterns.

2. Materials and method

2.1. Experimental design

Bovine cumulus oocyte complexes (COCs) were exposed to PFOS for 22 h during the final stage of maturation *in vitro* using two different concentrations. Bovine COCs (n = 1,945) were collected from abattoir-derived ovaries, randomly divided between exposed and control group, and subsequently kept separated during all following *in vitro* experiments. COCs (average 26, range 19–47) were matured, fertilised and cultured *in vitro* until day 8 post fertilisation (pf) under serum-free conditions. Developmental parameters were assessed during embryo culture (embryos cleaved and embryos cleaved beyond 2-cell stage 44 h pf, embryo development at day 7 and 8 pf, as well as stage and grade of developed embryos at day 7 and 8 pf).

At day 8 pf, blastocysts were fixed and stained for evaluation of blastomere count and lipid content using a confocal microscope (n = 78) or individually snap-frozen and pooled with 10 embryos in each group for later RNA and DNA extraction (n = 120). Four replicates for each experimental group were used for gene expression and DNA methylation analyses (Fig. 1).

2.2. Media and chemicals

Media were produced at the IVF laboratory at the Department of Clinical Sciences (Swedish University of Agricultural Sciences, Uppsala, Sweden) according to standard protocols (Gordon, 1994) as described previously in related projects at the facilities (Abraham et al., 2012; Hallberg et al., 2019; Laskowski et al., 2017). All chemicals and media used were purchased from Sigma Aldrich (Stockholm, Sweden) unless otherwise stated, details can be found in Tables S1 to S6 of the supporting information (SI).

PFOS (CAS no 1763-23-1, 77282, potassium salt ≥98.0 %) dissolved in molecular grade water (due to concentrations not exceeding water solubility of PFOS no vehicle other than water was used) was added to maturation media of the exposed groups to achieve 100 ng mL^{-1} and 10 ng mL^{-1} respectively. In the control, only vehicle (water) was added. PFOS stock solutions were stored at 4 °C protected from light; we did not expect degradation during the course of the experiments due to persistence of the compound. Due to PFOS loss during filtration of media, the final concentration was 2 ng mL^{-1} and 53 ng mL^{-1}, which is approximately 2–5 times under the intended dose, for details see Section 2.3. After *in vitro* maturation, media was frozen in −20 °C and samples of media stored for later analyses.

2.3. Validation of exposure concentration

Samples from the maturation media (one sample from the control, three samples from for PFOS-02 and PFOS-53 respectively) were sent for quantification of PFOS concentration to SGS, Linköping, Sweden. Due to protein content (bovine serum-albumin, BSA), analysis procedure was set up based on in-house methods and as described by Gyllenhammar et al., 2017 for serum samples (Gyllenhammar et al., 2017) with small modifications. Samples (0.5 g) were weighted into 12 mL centrifuge

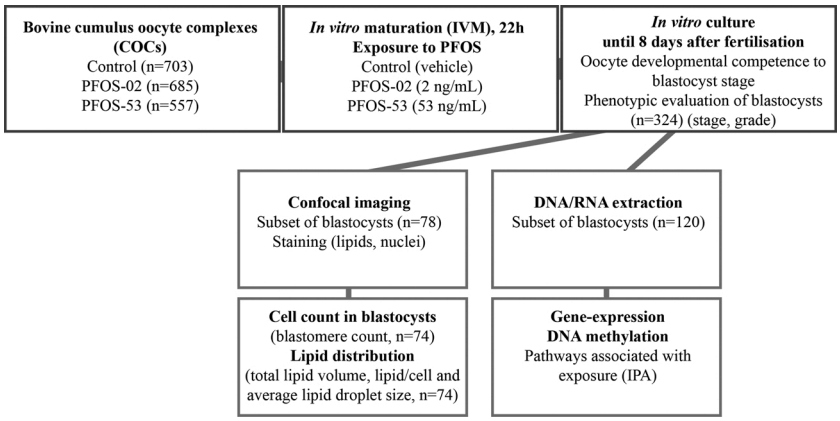

Fig. 1. Overview of the experimental design. Bovine oocyte cumulus complexes (COCs) were retrieved from the slaughterhouse after the animals have been killed. Exposure of PFOS occurred during *in vitro* maturation (IVM). Developmental competence of the oocyte to blastocyst stage were recorded during development until day 8 when phenotypic evaluation of the blastocysts were conducted. Stage and grade were evaluated using a light-microscope. A subset of blastocysts were stained for confocal imaging and DNA/RNA extraction for microarray analyses were performed on another subset of blastocysts (matched for stage and grade).

tubes of polypropylene and spiked with isotopically labelled internal standards. A blank and control were prepared in parallel to the media. After addition of acetonitrile for extraction, samples were vortexed-mixed, sonicated and centrifuged for 10 min at 2000×*g*. The extract was transferred to a new 12 mL centrifuge tube and the extraction procedure was repeated on the remaining media. The extracts were combined and diluted with molecular grade water and loaded onto weak anion exchange (WAX, Oasis® WAX6 mL, 6 mL, 500 mg, 60 µm, Waters) which was preconditioned with 0.1 % NH_4OH in methanol, methanol and water. The cartridges were rinsed with 1% formic acid in water, water and 0.1 % formic acid in methanol and then dried under vacuum. The samples were eluted with methanol and 0.1 % NH_4OH and the cartridges were dried under vacuum. Following evaporation of the eluates using N_2 steam, the extracts were dissolved in methanol and further diluted in ammonium acetate before being analysed using a LC–MS/MS system (Agilent 1290 Infinity II/6495A). Results were adjusted to blank signal and internal standard recoveries were used to compensate for potential loss during processing. In the media from the control, the PFOS concentration was below detection limit (<0.1 ng g^{-1}). In PFOS-02 the concentration of PFOS was 2.05 ng g^{-1} (range 2.0–2.1 ng g^{-1}) and in PFOS-53 the concentration was 53 ng g^{-1} (52−54 ng g^{-1}) which is the equivalent of 4 nM and 106 nM PFOS respectively (details can be found in supporting information, SI, Table S7). The lower concentration is equal to concentrations measured in human follicular fluid (Kim et al., 2020). The higher concentration is within the range of human relevance (Kang et al., 2020; Petro et al., 2014).

2.4. Bovine in vitro embryo production (IVP)

2.4.1. Oocyte recovery, in vitro maturation and exposure to PFOS

Bovine *in vitro* embryo production (IVP) was performed according to standard protocols (Gordon, 1994), and as previously described in related projects from our facilities (Abraham et al., 2012; Hallberg et al., 2019; Laskowski et al., 2016). Abattoir-derived ovaries from non-stimulated heifers and cows were collected and transported at 29 °C (range 28–30) within 3 h to the IVF laboratory facilities (Department of Clinical Sciences, Swedish University of Agricultural sciences, Uppsala). As the animals were not killed for the sake of this experiment, no ethical permission was required according to Swedish legislation. Acceptable COCs (compact multilayer cumulus investment and homogenous ooplasm, selection criteria according to (Gordon, 2003)) were randomly and equally distributed between the treatment/exposure groups.Incubation for 22 h for *in vitro* maturation followed, in bicarbonate buffered tissue culture medium 199 (TCM 199) supplemented with 0.68 mM L-Glutamine, 0.4 % w/v bovine serum albumin (BSA), Fraction V, 0.5 µg mL^{-1} FSH, 0.1 µg mL^{-1} LH (Stimufol, PARTNAR Animal Health, Stoumont, Belgium) and 50 µg mL^{-1} gentamicin sulfate (Table S2, SI). PFOS was added to the exposed groups and vehicle to the control in a volume of 10 µL mL^{-1}.

2.4.2. In vitro fertilization and culture

After maturation *in vitro*, presumed MII oocytes were co-incubated for 22 h with spermatozoa at a concentration of 10^6 mL^{-1} in fertilisation media (modified HEPES-buffered glucose-free medium (Gordon, 1994) with the addition of 16 mM sodium DL-lactate, 50 µg mL^{-1} gentamicin sulfate, 3 µg mL^{-1} heparin, 3 µg mL^{-1} of pencillamine, 1 µg mL^{-1} hypotaurine and 0.3 µg mL^{-1} epinephrine (PHE-solution), Table S5, SI). One single ejaculate from a single bull with proven *in vitro* and *in vivo* fertility was used for all replicates. Presumed zygotes were then washed to remove excessive spermatozoa and cumulus cells and cultured until day 8 pf in modified synthetic oviductal fluid (mSOF, Table S6, SI) with the addition of 0.4 % w/v fatty acid free BSA, 20 µg mL^{-1} BME amino acids solution (50×) and 10 µg mL^{-1} MEM non-essential amino acids solution (100×), with wells covered in OVOIL™ (Vitrolife, Göteborg, Sweden).

2.5. Phenotypic evaluation of embryos after PFOS exposure

2.5.1. Evaluation of developmental competence to blastocyst stage

During IVP, developmental parameters were assessed as previously described (Hallberg et al., 2019). At 44 h pf, cleaved zygotes and zygotes cleaved beyond 2-cell stage were recorded. At day 7 and day 8 pf, proportion blastocysts as well as morphology and developmental stage of the embryos were recorded. The stage was assessed according to IETS grading system developed for assessing bovine embryos for trade, transfer and research (IETS, 2010), but modified into 3 stages; early blastocyst or blastocyst stage (stage 1). Expanding or expanded blastocysts where the zona pellucida has thinned due to blastocysts expansion (stage 2) and hatching or hatched blastocysts, where zona pellucida has started to or ruptured (stage 3). The quality of each embryo was graded according to IETS grading scheme (IETS, 2010) from grade 1–4, where grade 1 corresponds to a top quality embryo. An embryologist trained in the grading scored the embryos, and within the same replicate the same person scored all embryos but were not blinded to the treatments, as the practical laboratory work did not allow this.

2.5.2. Fixation and staining of blastocysts

Blastocysts from day 8 pf (n = 78) were fixed in 2 % paraformaldehyde at 4 °C overnight, followed by rinsing in phosphate buffered saline with 0.1 % polyvinyl alcohol (PBS-PVA). DNA was visualized by fluorescent labelling of DNA in 2.5µM Hoechst 33342 (B2261) incubated in RT for 15 min and rinsed with PBS-PVA followed by staining for visualising neutral lipids using LipidTOX™ (HCS LipidTOX™ Green Neutral Lipid Stain H34475, Thermo Fisher Scientific, Waltham, USA) for 30 min at RT according to the manufacturer's

instructions. To ensure absence of background fluorescence, a negative control accompanied the blastocyst during the staining procedures but was excluded from fluorescent labelling. Embryos were mounted on a microscope-slide (ER-201B-CE24, Thermo Fisher Scientific) in approximately 2 μL Vectashield (Vector Laboratories Inc., CA, US).

2.5.3. Confocal microscopy and image analysis

Stained embryos (n = 78) and negative control embryos (n = 3) were scanned using standard magnification (20×) in sections at 2 μm intervals (z-stack) using a confocal microscope (Zeiss LSM 800) equipped with He/Ne 543 and Ar 450/530 lasers. All steps of image processes were performed by an operator blinded to the codes and thereby the treatments of the individual blastocysts. Negative controls did not show detectable florescence. Images were analysed using Fiji for ImageJ (https://imagej.net/Fiji/) software. To separately detect nuclei and lipids in their respective colour channels, a local adaptive threshold approach was used that computes the optimal threshold level for each object to optimise an ellipse fit (Bombrun et al., 2017; Ranefall et al., 2016). The channels were aligned in each section as well as between sections. Random background noise (due to intensity threshold used for the signal detection) was reduced by applying a quality check based on the general stain after the normalisation. After computed-assisted image analysis, the results were manually validated by operator blinded to the codes, and images were excluded when extensive deviations were recorded, *i.e.* when the macro failed to recognise lipids and/or nuclei because of image quality (n = 4). The average volume of all lipid droplets within an embryo (average lipid droplet size, μm^3); the sum of all lipid droplet volume in each embryo (total lipid volume, μm^3); and total volume of lipids divided by number of cells (lipid volume/cell, μm^3) were recorded.

2.6. Statistical analysis

RStudio for R (R i386, 4.0.5,) was used for statistical comparisons. The effect of treatment on developmental parameters (proportion of cleaved, cleaved beyond two-cell stage and blastocysts on day 7 and day 8) was calculated using mixed effect logistic regression with binary distribution with replicate as a random factor and weighted for group size to calculate the odds ratio (glmer model of the lme4 package, R i386, 4.0.5). Day 7 and day 8 blastocysts were treated as repeated measurements and therefore results for blastocyst development are presented as one outcome (glmmSQL model of the MASS package, R i386, 4.0.5). Odds ratio (OR) <1 indicate a negative effect of treatment. The effects of treatment on ordinal variables (stage, grade) were analysed using cumulative link mixed-effect models with multinomial distribution (clmm model of the ordinal package, R i386, 4.0.5) with replicate as random factor. This resulted in one model for effect of treatment on stage. Linear mixed effect models (lmer model of the lme4 package, R i386, 4.0.5) were used to calculate the effect of treatment on the continuous variables total lipid volume, average lipid droplet size, and lipid volume/cell. Replicate (random factor) and treatment (fixed factor) were included in the models. Due to the high energy-demand in the transition from morula to blastocyst-stage, the lipid content is decreased in blastocysts (Sudano et al., 2016). Therefore, it is expected that lipid content is different in different blastocyst-stages. To account for this difference, stage (fixed factor) and blastomere count (fixed factor) and their interactions were considered for inclusion in the models for lipid distribution. Stage and blastomere count were highly correlated, and therefore only stage was included in the final models based on best model fit. The interactions were removed based on p-values and model AIC. Blastomere count provided an objective and blinded measurement of blastocyst size (and indirectly stage). The results from this model are therefore also presented in addition to the model of blastocyst stage. The effect of treatment on blastomere count in blastocysts at day 8 blastocysts was calculated using linear mixed effect models with replicate as a random factor. For degraded embryos or embryos not reaching blastocyst stage, square root transformed values were used to obtain normal distribution. Results are presented as mean ± SEM if not stated otherwise and $p < .05$ were considered significant.

2.7. Gene-expression and DNA methylation analyses

2.7.1. Parallel gDNA and total RNA extraction

Blastocysts from day 8 pf (n = 120) were individually snap-frozen in liquid nitrogen in a fixed volume of PBS-PVA. The embryos were then stored in −80 °C until further analysis. Pools of 10 embryos of equivalent stage and grades (in order to avoid confounding effects due to different embryo characteristics) were analysed in four replicates for both controls and treated groups (see SI Table S8 for details on groups). Parallel genomic (g)DNA and total RNA extraction was conducted using the AllPrep DNA/RNA micro kit (Qiagen Cat no 80284) according to the manufacturer's instructions with slight modifications (Page-Lariviere et al., 2017). Washed DNA was eluted in elution buffer, evaluated using NanoDrop (ND-1000, NanoDrop Technologies, Wilmington, DE, USA) and stored at −80 °C for further use. RNA was eluted in 15 μL RNAse-free water and purity, quality and concentration were evaluated using the Agilent Bioanalyzer 2100 (Agilent technologies Inc., Santa Clara, CA, USA) where all samples had an RNA integrity number ≥8.9 (range 8.9–9.7) which was considered as good quality. RNA was stored at −80 °C.

2.7.2. RNA amplification and microarray hybridisation

RNA was amplified using the 2-round RiboAmp® HS^{PLUS} RNA Amplification kit (Applied Biosystems, Foster City, California, USA), which provides amplification of small amounts of RNA and yields sufficient material (antisense (a)RNA) for microarray hybridisation using a T7 RNA polymerase amplification approach (T7-IVT). Amplified aRNA was quantified (Nano-Drop ND-1000, NanoDrop Technologies, Wilmington, DE, USA) and labelled with Cy3 and Cy5 using the Universal Linkage System (ULS™) Fluorescent Labelling Kit (Leica, Wetzlar, Germany). Exposed groups (PFOS-53 and PFOS-02) were compared to the control using a four-array dye-swap design. For a duration of 17 h at 65 °C, 825 ng aRNA per replicate was hybridised to an Agilent-manufactured EmbryoGENE slide in 10× blocking agent and 25× fragmentation buffer (Agilent). After hybridisation, the slide was washed (0.005 % Triton X-102 repeated twice followed by acetonitrile and drying and stabilising solution, provided by Agilent) and scanned using a PowerScanner (Tecan Group Ltd., Mannedorf, Switzerland). Feature extraction was performed with Array-pro 6.3 (Media Cybernetics, Rockville, Maryland, USA).

2.7.3. Analysis of gene expression profile

In the microarray, 42,242 probes were covered including 21,139 reference genes, 9,322 probes for novel transcribed regions, 3,677 alternatively spliced exons, 3,353 3′-tiling probes and 3,723 control probes (Robert et al., 2011). Relative transcript abundance was analysed using Flexarray (Blazejczyk et al., 2007). Background was subtracted from the raw fluorescence intensity. Normalisation within the fluorophores (Cy3/Cy5) and between each array was conducted using Loess and quantile respectively. Comparison between treatments (exposed groups and control) was performed with the limma algorithm. Each probe was attributed a probability to fold-change between treatment and control and differentially expressed genes (DEGs) defined as significant ($p < .05$) probes with fold change > 1.5. Applying fold change or false-discovery rate (FDR) by Benjamini Hochberg correction did not generate enough transcripts for pathway analysis. All significant probes ($p < .05$) were therefore analysed by Ingenuity Pathway analysis (QIAGEN Ingenuity Pathway Analysis (IPA) software). In order to obtain a general overview of pathways affected on transcriptomic level, all significant ($p<0.05$) transcripts were included. The IPA analysis consider the amount of transcripts consistent with the effects and adjust

its p-value accordingly. In this way, if several transcripts are linked to the same pathway in the same direction, this represent more important information at the cellular level and the analysis gives higher significance/importance to it.

2.7.4. gDNA fragmentation, amplification and hybridisation

gDNA from the same pools used for transcriptome microarray was amplified and enzyme fragmented before hybridisation for Agilent arrays as described previously (Saadi et al., 2014). The gDNA was fragmented using MseI enzyme (NEB-R0525S) to enable standardised fragmentation between experiments regardless of methylation status. gDNA was then treated with methylation sensitive enzymes (AciI (NEB-R0551S), Hinp1I (NEB-R0124S), HpaII (NEB-R0171 L)) to enable fragmentation according to methylation status, whereby methylated regions are protected from cleavage. After enzymatic digest, samples were amplified by ligation-mediated PCR resulting in exponential amplification of the methylated regions. Labelled (Cy3/Cy5) samples of exposed groups (PFOS-02 and PFOS-53) were compared to the control using a four-array dye-swap design. Hybridisation was performed according to the manufacturer of the microarrays instruction (Agilent). Labelled samples were hybridised in 100× Blocking agent and 2× hybridisation buffer (Agilent) and for 40 h at 65 °C. Hybridised samples were then washed according to the manufacturer's instructions and scanned with the PowerScanner (Tecan) and features were analysed using Array-Pro Analyser 6.3 Software (Media Cybernetics).

2.7.5. Quantification of DNA methylation patterns

The bovine EmbryoGENE DNA Methylation Array (EDMA) was used to analyse the DNA methylation patterns of the embryos as previously described (Montera et al., 2013; Saadi et al., 2014). The microarray containing methylation sites within the bovine genome without topological bias contained a total of 414,566 probes, surveying 20,355 genes and 34,379 CpG islands. Controls accounted for 2.5% of the total probe number and represented Agilent proprietary controls, genomic cleavage controls and EDMA spiked-in controls (Saadi et al., 2014). Quantile inter-array scale normalisation followed loess intra-array normalisation within the limma-package of a pipeline described previously to obtain Bayesian statistics of different methylations, including controls and validations (Saadi et al., 2014). For comparative analyses, differentially methylated regions (DMRs) were defined when $p < .05$ and fold change > 1.5. Functional analysis was performed by IPA on significantly different probes ($p < .05$) without applying fold change or FDR adjustment to analyse altered pathways after PFOS exposure (see Section 2.7.3).

3. Results

3.1. Oocyte developmental competence until blastocyst stage after exposure to PFOS during IVM

Exposure to 53 ng mL^{-1} PFOS during oocyte maturation *in vitro* significantly decreased the chance of the fertilised embryo reaching cleaved stage at 44 h pf, which was also observed as a reduced chance of cleaving beyond two-cell stage (Fig. 2, exact proportions, OR and *p*-values shown in Table 1). This was not observed in the PFOS-02 group. The initial delay in development in the PFOS-53 group could not be seen in later stages of early embryonic development. The proportion of embryos reaching blastocysts stage at day 7 or 8 did not differ from the control group (Fig. 2, Table 1). Phenotypic variation in blastocysts upon exposure to PFOS during IVM

3.1.1. Blastocyst stage and cell count

PFOS exposure led to impaired blastocyst development, whereby a smaller proportion of embryos reached more advanced stages at day 8 compared to the control (Fig. 3A). The reduction in stage was significant in PFOS-53 (p=.01) but not in PFOS-02 (p=.06). This corresponded to a reduced number of blastomeres in PFOS-53 (mean 70.1 (SEM 4.7) $p = .04$, Fig. 3B) compared to the control (84.8 (5.0)) in the subset of

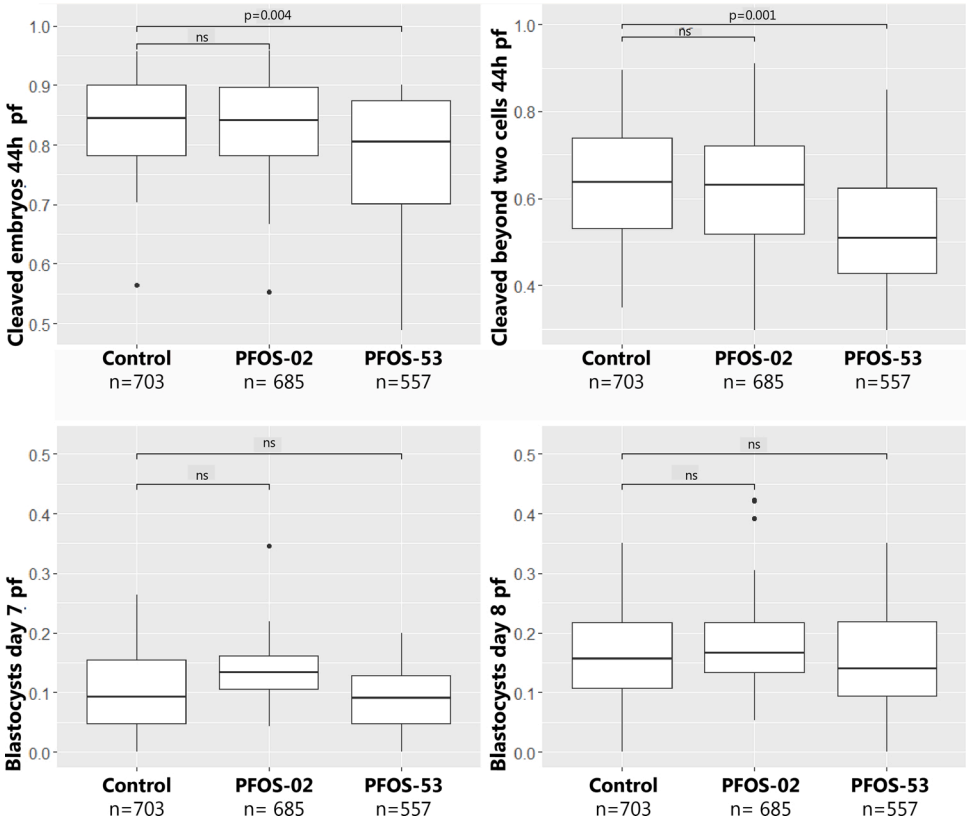

Fig. 2. Developmental competence of bovine oocytes after PFOS exposure during *in vitro* maturation. Boxplots showing the proportion of developed embryos in control and after treatment of oocytes with 2 ng mL^{-1} or 53 ng mL^{-1} PFOS (PFOS-02 and PFOS-53, respectively). Proportion of cleaved embryos and cleaved embryos beyond two-cell stage 44 h post fertilisation (pf), and proportion of blastocysts at day 7 and day 8 pf calculated from cultured oocytes are shown. The data are presented as boxplots where line represent median, the box is the interquartile range (IQR), and whiskers are 1.5 × IQR, outliers depicted with dots and represent values > 1.5 × IQR. Non-significant *p*-values annotated with ns.

Table 1
Developmental competence of oocytes after exposure to PFOS during maturation *in vitro*.

	Control (n = 703)	PFOS-02[a] (n = 685)			PFOS-53[b] (n = 557)		
	Proportion[c] (±SEM)	Proportion (±SEM)	Odds ratio (CI)[d]	p	Proportion (±SEM)	Odds ratio (CI)	p
Cleaved[e]	0.83 (0.01)	0.83 (0.01	1.08 (0.82–1.42)	.55	0.76 (0.02)	0.67 (0.51–0.88)	.004
Cleaved beyond 2-cell stage[e]	0.63 (0.02)	0.63 (0.02)	1.01 (0.81–1.25)	.96	0.53 (0.03)	0.69 (0.55–0.87)	.001
Blastocyst rate day 7	0.12 (0.01)	0.15 (0.01)	1.24 (0.89–1.74)[f]	.19	0.08 (0.01)	0.73 (0.50–1.07)[f]	.10
Blastocyst rate day 8	0.19 (0.01)	0.20 (0.02)			0.14 (0.02)		

[a] Two ng mL^{-1} PFOS during *in vitro* maturation.
[b] 53 ng mL^{-1} PFOS during *in vitro* maturation.
[c] Calculated from the number of cultured oocytes at the start of the experiment.
[d] Odds ratio and confidence interval (CI) calculated by logistic regression.
[e] Cleaved and cleaved beyond two-cell stage assessed 44 h after fertilisation.
[f] Day 7 and 8 blastocyst rates were considered repeated measurements resulting in one outcome from the model.

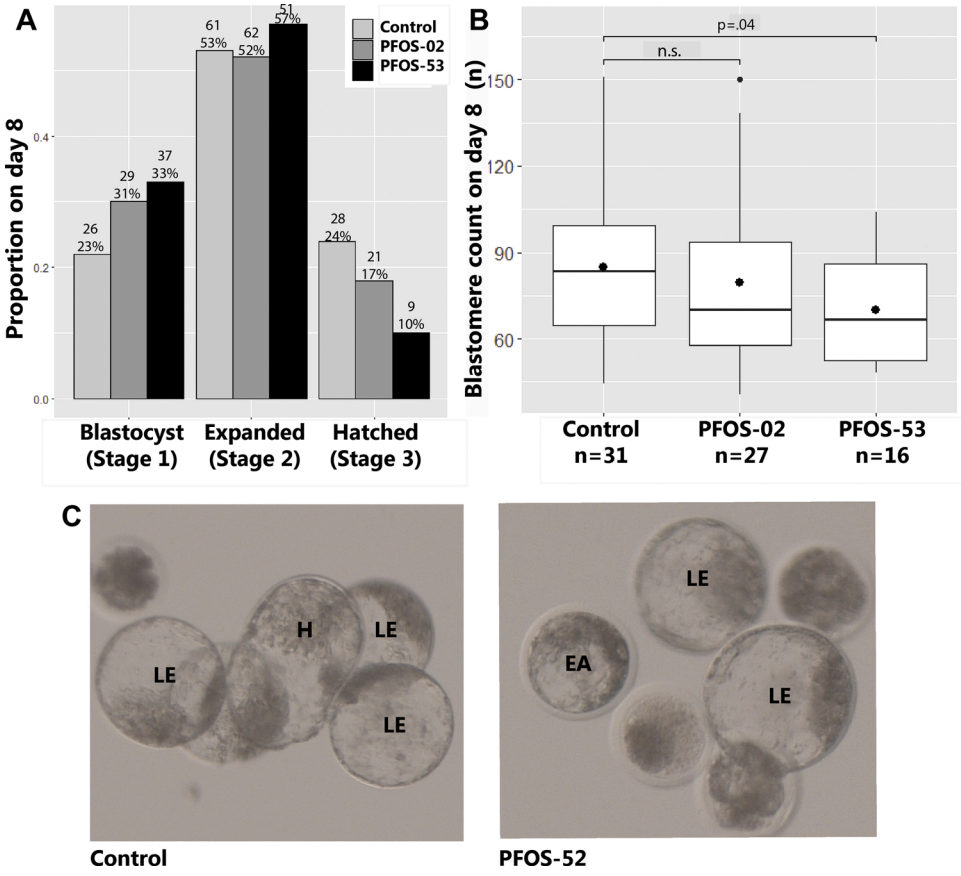

Fig. 3. Stage and blastomere count in day eight blastocysts after PFOS exposure during oocyte maturation. A, proportion of blastocysts in different developmental stages in each treatment, the proportion out of total blastocyst in each category, as well as numbers of blastocysts are presented above each bar. The stage in PFOS-53 was lower compared to the control in a cumulative mixed-effect model to calculate the effect of treatment on developmental stage (p=.01) but not in PFOS-02 (p=.06). B, amount of blastomeres in blastocysts. Data presented as boxplots where the line represents the median, the box is the interquartile range (IQR), and whiskers are 1.5 × IQR, outliers depicted with dots and represent values > 1.5 × IQR. The decreased number of blastomeres was significant from the control in PFOS-53 (p=.04) but not in PFOS-02 (p=.70). Light microscope images of representative embryos showing how embryos in the control have progressed further in development to more advanced developmental stages (H = hatching, LE = late expanding, EA = early expanding).

embryos stained for confocal imaging. There was no difference in blastomere count in the PFOS-02 group (79.5 (5.5) p=.70) compared to the control. The embryos that did not develop into blastocyst stage or were degraded at day 8 pf were also assessed for blastomere count. There was no difference in how far the development proceeded (mean nuclei in control 7.8 (SEM 0.4), PFOS-02 7.9 (0.4), p=.63, PFOS-53 8.0 (0.4), p = .56). We can observe that the oocytes not developing into blastocyst stage halt development at an early stage, before embryo genome activation (8–16 cell stage in bovines, (Barnes and First, 1991)).

The quality grade of the embryos, scored according to the IETS system, was not altered by PFOS treatment (PFOS-53 p = .20, PFOS-02 p = .69).

3.1.2. Lipid distribution in blastocysts

To evaluate lipid storage and metabolic status of the blastocysts, lipid distribution (average lipid droplet size, total lipid volume, lipid volume/cell) was measured in the blastocysts. Blastocyst size were added in the models to account for differences in lipid content depending on developmental stage (see Section 2.6 for detail). Blastocysts that developed from oocytes exposed to PFOS during *in vitro* maturation showed an increased lipid volume/cell in PFOS-53 (control: mean 607.6 (SEM 44.3) μm^3, PFOS-53: 853.0 (91.4) μm^3, $p <$ .0001) as well as an increased total volume of lipids in the embryo (control 53371 (5678) μm^3, PFOS-53 61543 (9251) μm^3, p=.0003) (Fig. 4). This was not seen in the PFOS-02 group (lipid volume/ cell 621.1 (57.3) μm^3, p=.62 and total volume of lipids in the embryo 50175 (6212) μm^3, p=.65). However, the average lipid droplet volume was lower in PFOS-02 (39.09 (3.3) μm^3, p=.02) compared to the control (46.09 (4.0) μm^3), a characteristic not detected in PFOS-53 (51.40 (5.75) μm^3, p = .84) (Fig. 4).

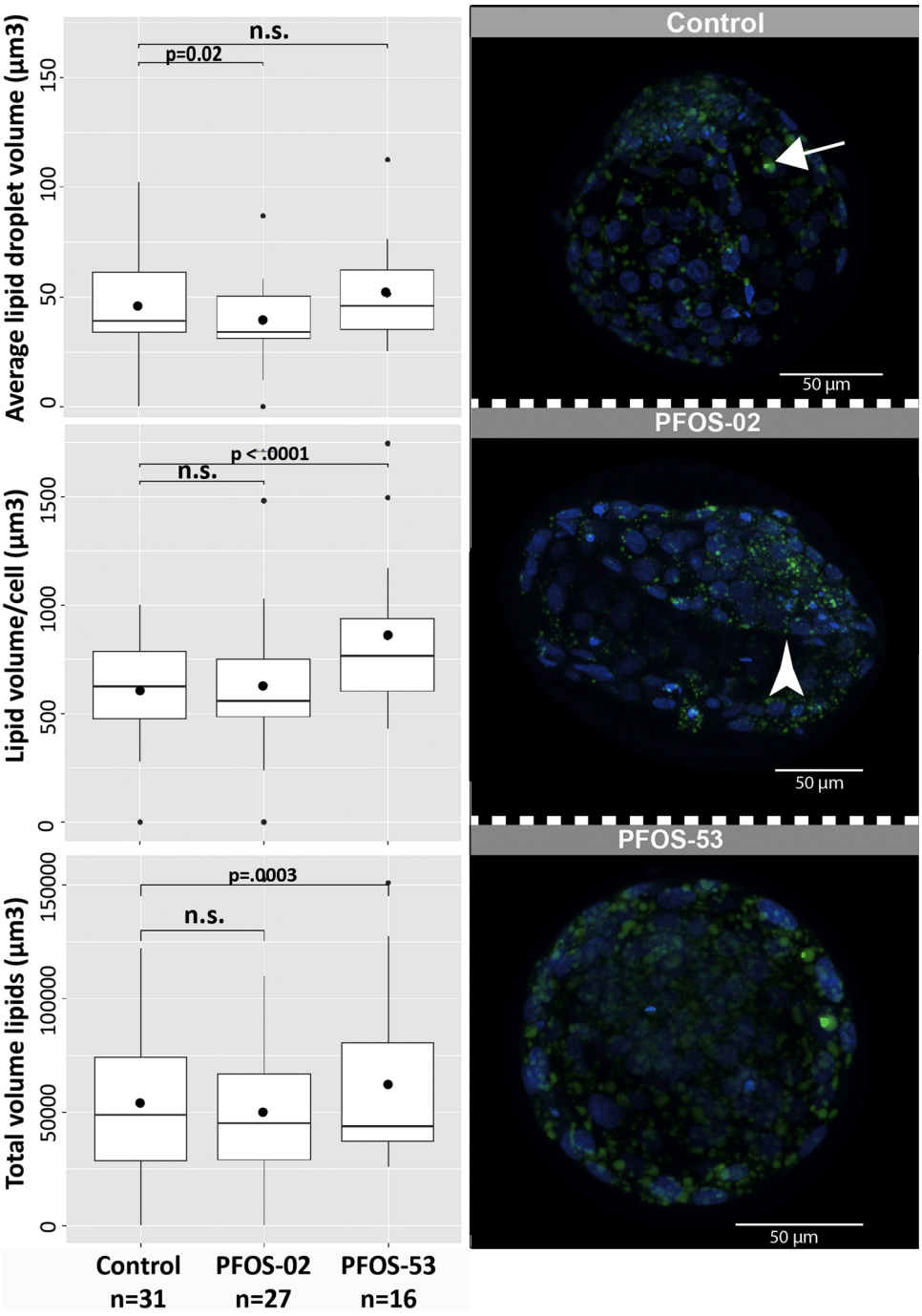

Fig. 4. Variation in lipid distribution after PFOS exposure. Boxplots showing lipid distribution in the embryos after PFOS exposure during oocyte maturation (average lipid droplet volume, lipid volume/cell and total volume lipids, um^3), *p*-values $< .05$ are shown and values not significant are indicated by n.s. The data are presented as boxplots where the line represents the median and bullet the mean, the box is the interquartile range (IQR) and the whiskers are $1.5 \times$ IQR. Outliers are depicted with dots and represent values $> 1.5 \times$ IQR. Confocal imaging of day eight blastocysts stained for neutral lipids (LipidTOX, green) and nuclei (Hoechst, blue) showing representative embryos from the control and the PFOS treated groups. Note larger lipid droplets in embryos from control (arrow) compared to PFOS-02 group (arrowhead). Note also the increased amount of total lipids in PFOS-53 compared to the control.

3.2. Gene expression changes in blastocysts upon oocyte exposure to PFOS during IVM

To determine the changes in gene expression after PFOS exposure during IVM, transcriptomic analyses using microarrays on pools of day eight blastocysts of equivalent stage and grade (to avoid confounding effects from different embryo characteristics at different stages of development) were performed. Following Benjamini-Hochberg adjustment of *p*- values, for multiple comparisons, no differentially expressed genes (DEGs) were identified. When applying fold change threshold to non-adjusted *p*-values, 16 DEGs (fold change > 1.5, $p < .05$) were identified in PFOS-02, of which 12 were downregulated and four upregulated (Fig. 5A). In PFOS-53, 223 DEGs (fold change > 1.5, $p < .05$) were found, with the majority being downregulated (218) and five genes upregulated (Fig. 5B). Five genes overlapped between the treatments (Fig. 5C). The transcripts differentially expressed in both treatment were *ubiquitin D (UBD),* which was upregulated and *Histone H2B type 1-N (HIST1H2BN), sperm-adhesion molecule-1 (SPAM1), transcription factor 15 (TCF15)* and *charged multivesicular body protein 4B (CHMP4B)*, all downregulated (Fig. 5D).

3.2.1. Functional analysis of gene expression changes

In a functional analysis of gene expression changes in PFOS treated groups compared to control, DEGs with > 1.5 fold change in expression and $p < .05$ (16 for PFOS-02 and 223 for PFOS-53) showed no enrichment for specific biological functions using Ingenuity pathway (IPA) analysis. Instead, in order to obtain a general overview of pathways in the blastocysts associated with oocyte exposure, we considered also

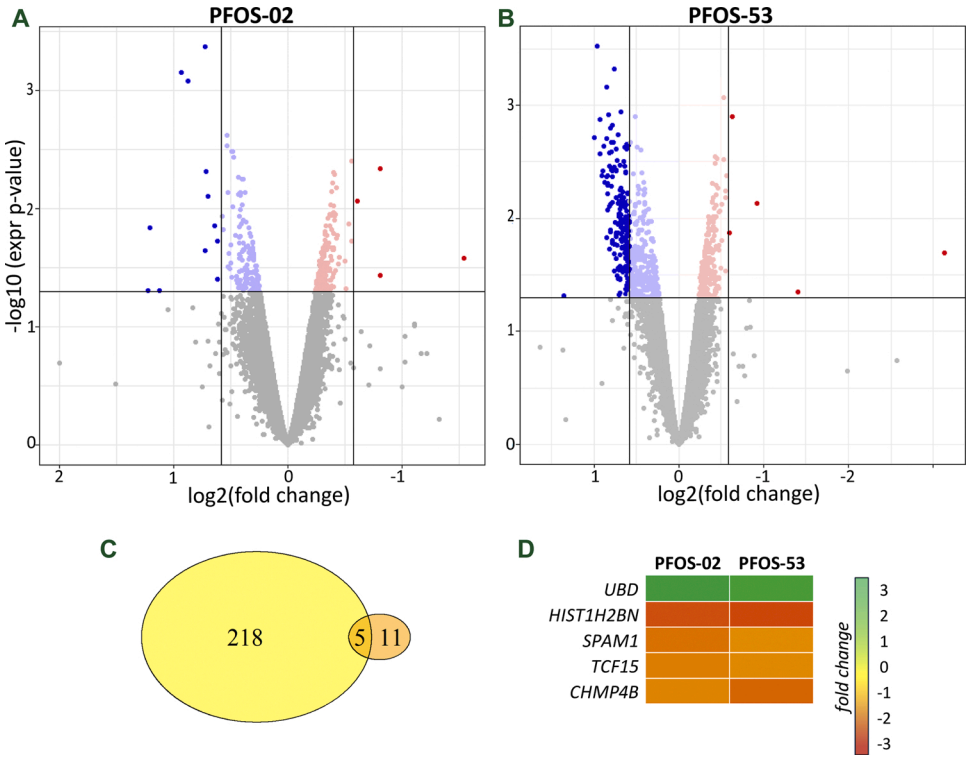

Fig. 5. Gene expression relative to control in day eight blastocysts following treatment with PFOS during oocyte maturation *in vitro*. Volcano plot of fold changes and *p*-values illustrating in PFOS-02 (A) and PFOS-53 (B). Blue indicates downregulated genes (light blue = $p < .05$, dark blue = fold change > -1.5, $p < .05$) and red upregulated genes (light red = $p < .05$, dark red = fold change > 1.5, $p < .05$). Venn-diagram (C) showing DEGs (fold change > 1.5, $p < .05$) in PFOS-53 (yellow) and PFOS-02 (orange) and overlap. Five transcripts were differentially regulated (fold change > 1.5, $p < .05$) in both microarrays (D).

small changes in expression if transcripts belonged to the same biological pathways. Using this larger set of genes (n=668 in PFOS-53, n=300 in PFOS-02), IPA analysis revealed the top biological functions altered after PFOS treatment at both doses to be related to proliferation, cell death and survival, cell differentiation, export and transport of RNA or proteins, and initial expression or transcription of RNA. There was a higher number of transcripts included in each biological function for PFOS-53 (668) compared to PFOS-02 (300). This resulted in an overall stronger prediction of altered biological functions in the higher concentration (Fig. 6).

Regulatory pathways upstream of the significant transcripts ($p < .05$, no fold change criteria) were identified by IPA. This analysis revealed pathways differently regulated in PFOS-treated groups, compared to the control group, which were related to apoptosis, cell stress and metabolism. Alterations were more pronounced in the PFOS-53 group compared to the PFOS-02 group (full table of activated and inhibited upstream regulators can be found in SI, Tables S9 and 10). More specifically, both treatments were predicted to alter biological functions related to cell death and survival which occurred most significantly through *P38 MAPK* (Fig. 6, PFOS-53*: z-score −2.3, p = .001, 23 transcripts,* PFOS-02*, z: −2.9, p = .04, 10 transcripts)* and *STAT 3* (PFOS-53*: z: −3.1, p = .002, 21 transcripts,* PFOS-02*, z: −1.9, p = .02, 15 transcripts)* inhibition. This was observed for both treated groups leading to *TP53* activation and apoptosis (biological function: *Apoptosis,* PFOS-53*: p = 1.85e-09, 50 transcripts,* PFOS-02*: p = 3.56e-03, 75 transcripts)*. Furthermore, pathways associated with embryo response to stress and metabolic stress response were altered in both treatments, but most significantly in PFOS-53. Altered metabolisms with overlap to metabolic stress response were seen through *NONO (e.g., ACACA, FASN), INS1 (e.g., APOA1)* and *APOE (i.e. APOA1, FOS)* activation and *JUN (e.g., CAV1, PTEN)* inhibition. Metabolic biological functions altered in PFOS-53 included decreased synthesis of lipids (*p = 2.25e-05, 6 transcripts)* and altered concentration of lipids (*p = 3.45e-04, 579 transcripts)*. Embryo response to stress was predicted to occur through alteration of biological functions related to the generation of reactive oxygen species (ROS) (*p = 2.03e-04, 621 transcripts)* and metabolism of ROS (*p = 2.04e-05, 159 transcripts*), and oxidative stress response (*p = 5.53e-04, 252 transcripts)* in PFOS-53.

CTNNB1 and *RELA* inhibition was as also predicted to be inhibited after exposure to PFOS-53. These pathways, as well as *STAT3*, are pathways with functions that include embryo development and blastocyst formation.

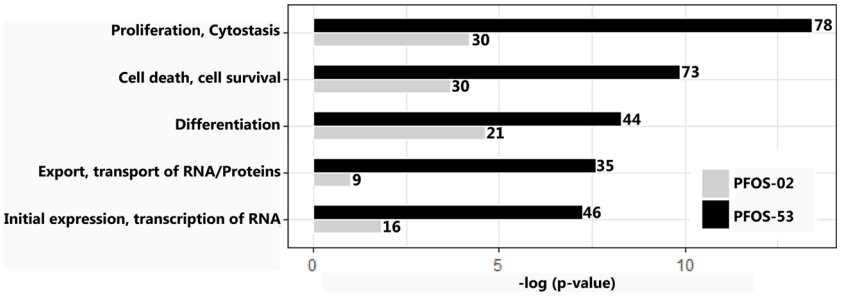

Fig. 6. Enrichment of top five molecular biofunctions altered after both PFOS exposures (PFOS-53 and PFOS-02) compared to control, derived from IPA analysis of all significant differentially expressed transcripts regardless off fold change and ranked by *p*-values (lowest to highest) in PFOS-53. –log(*p*-values) of the top functions are presented. The number to the right of each bar represents the amount of transcripts predicting the function.

3.3. Assessment of DNA methylation patterns

In order to address if PFOS treatment affected DNA methylation, and whether this could be linked to transcriptional changes, the same groups of pooled day eight blastocyst as used in the transcriptomic microarray were analysed using the Agilent EDMA microarray. When applying a Benjamini Hochberg adjustment of *p*-values, no DMRs were identified. Using unadjusted p-values, 189 DMRs were identified in the PFOS-53 group (fold change >1.5, $p < .05$), of which 69 were hypermethylated and 120 hypomethylated. In the PFOS-02 group, 380 DMRs were identified, of which 81 were hypermethylated and 299 hypomethylated (Fig. 7). In PFOS-02, one probe was identified as both DMR and DEG; *uromodulin like 1 (UMODL1)*. For PFOS-53, there were four probes identified as both DEGs and DMRs, namely *neurexin 2 (NRXN2), Interleukin-2 receptor alpha (IL2RA), zinc finger protein 532 (ZNF532)* and *methyl CpG binding protein 2 (MECP2)*. There were 83 and 193 significant ($p < 0.05$) probes overlapping between the transcriptomic and DNA-methylation microarray for PFOS-02 and PFOS-53, respectively (Fig. 8).

The difference in methylation was less prone to occur in proximal promoter regions (PFOS-02 p=.004, PFOS-53 p=.02) than expected, while there was an enrichment of DMRs in exonic regions (PFOS-02, $p = 0.05$, PFOS-53, $p < .001$). PFOS-02 and PFOS-53 DMRs were enriched in CpG-shores and CpG islands, respectively, while depleted in open sea region ($p < .001$) (Figs. S1–S2, SI).

3.3.1. Functional analysis of methylation changes

DMRs with > 1.5 fold change and $p < .05$ showed no enrichment for specific biological functions using Ingenuity pathway (IPA) analysis. Functional analysis was conducted where all significant genes between treated group and control regardless of fold change were taken into account. With the larger dataset (PFOS-02: 3,898, PFOS-53: 3,545), IPA revealed methylation changes that were associated with biological functions after PFOS treatment. The top biological functions were related to cell death and survival (PFOS-53: $p = 2.73e\text{-}22$, PFOS-02: $p = 9.73e\text{-}20$,), proliferation and cytostasis (PFOS-53: $p = 1.97e\text{-}18$, PFOS-02: $p = 1.42e\text{-}19$), differentiation (PFOS-53: $8.52e\text{-}13$, PFOS-02: $p = 4.62e\text{-}18$), transport of RNA and molecules ($3.22e\text{-}09$, PFOS-02: $p = 5.45e\text{-}16$), and transcription of RNA (PFOS-53: $p = 9.82e\text{-}09$, PFOS-02: $p = 3.00e\text{-}15$).

With the same data set, regulatory pathways upstream of the significant DMRs were identified by IPA. This analysis revealed pathways differently regulated in PFOS-treated groups compared to the control group that were similar between to the ones identified with the transcriptomic data set. Full data on upstream regulators of PFOS-02 and PFOS-53 can be found in Tables S11 and 12 in the SI. The most significantly affected pathway in both treatments was *TP53* signalling (PFOS-02: $p = 1.37e\text{-}18$, *248 loci,* PFOS-53: $p = 1.18e\text{-}18$, *448 loci)* which we had also identified in the transcriptome data set. *FASLG, NOTCH1* were examples of genes differently regulated in both the transcriptomic and DNA methylation data sets in PFOS-53. Altered *CTNNB1* regulation (PFOS-02 $p = 3.91e\text{-}06$, *194 loci,* PFOS-53 $p = 1.12e\text{-}16$, *183 loci)* and *TNF* regulation (PFOS-53, p=*1.37e-08*) were also persistent following PFOS-exposure and present in both methylation and transcriptomic data sets. For PFOS-53 treatment, 59 genes belonging to these 3 pathways were overlapping between the transcriptomic and DNA methylation data set (Table 2).

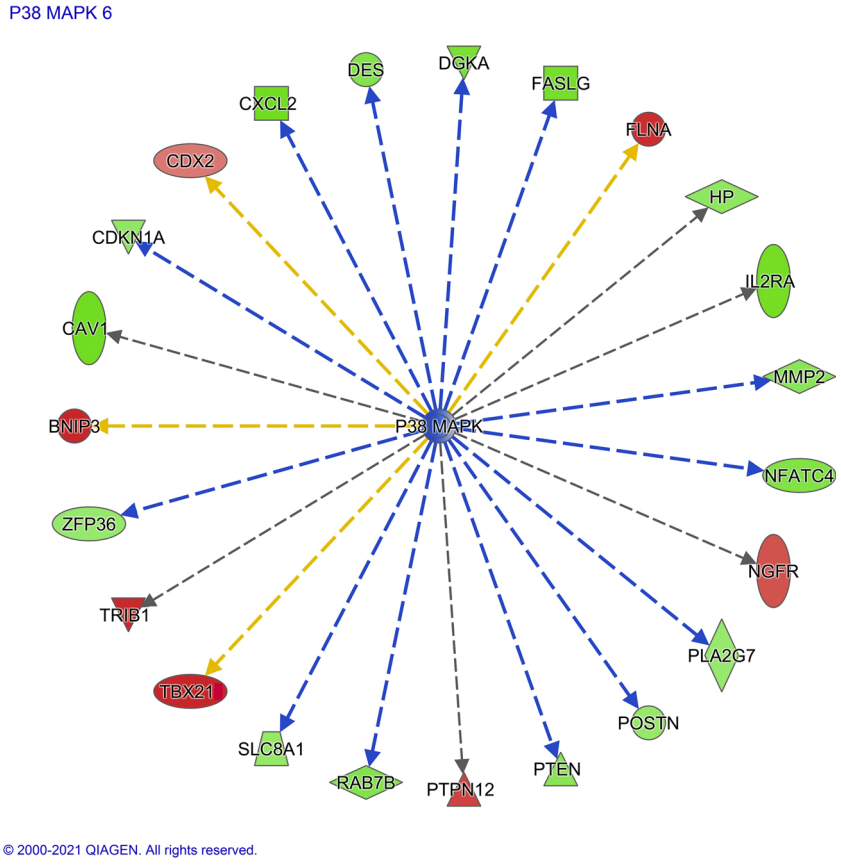

Fig. 7. Downstream signalling after upstream inhibition of P38 MAPK. Predicted inhibition of *P38 MAPK* signalling and transcripts associated with the prediction. Upregulated transcripts are in red and downregulated transcripts are in green. Arrows showing relationships where blue lead to inhibition, red to activation, yellow indicates findings inconsistent with state of downstream molecule and grey indicates when effect is not predicted.

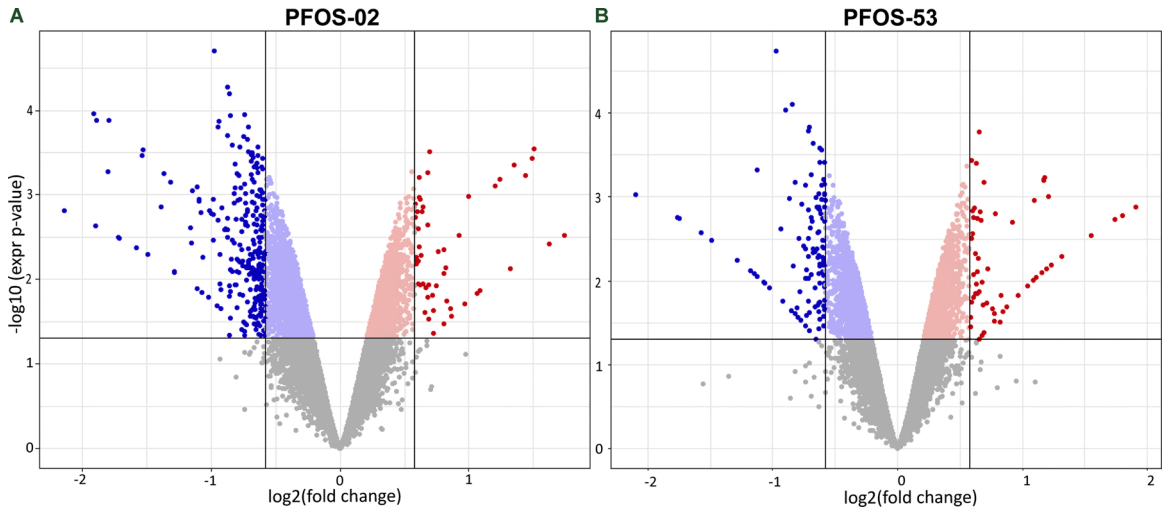

Fig. 8. Volcano plot of differentially methylated regions compared to the control in PFOS-02 and PFOS-53 respectively in the Agilent EDMA microarray. The y-axis represents –log10(expr *p*-value) and the x-axis log2(fold change) calculated based on different methylation assessed from methylation-sensitive enzymes.

4. Discussion

4.1. Exposure relevant to humans

In the present study, we show how exposure to human relevant concentrations of PFOS during a brief window of exposure during oocyte final maturation *in vitro* (IVM) alters early embryo development in a bovine model. Concentrations in maturation media were validated by mass-spectrometry (53 ng g^{-1} and 2 ng g^{-1}) and were lower compared to what has commonly been used in experimental *in vitro* settings. The concentrations reached were comparable to levels measured in follicular fluid in IVF cohorts (average range 2–7.5 ng mL^{-1}, range 0.6–30.4, (Heffernan et al., 2018; McCoy et al., 2017; Petro et al., 2014)), and the exposure in the *in vitro* setting thus simulated the exposure *in vivo* where the follicular fluid surrounded the oocyte during maturation in the mammalian follicle. Even though concentrations of PFOS in follicular fluid are lower compared to serum, the transfer efficiency to follicular fluid is close to one (0.64,) suggesting that serum concentrations in the general public can also be used as an estimate to oocyte exposure. PFOS-02 exposure was generally lower than the average exposure measured in human serum and PFOS-53 approximately ×1-10 higher than levels measured in the general public (Calafat et al., 2007; Kärrman et al., 2007; Mamsen et al., 2017; Velez et al., 2015; Wikström et al., 2020). In addition, local contamination of ground water depots used as drinking water sources may have led to exposures that clearly exceeded the levels measured in the general public. For example, the average serum level in the heavily exposed Ronneby community in Sweden is 245 ng mL^{-1} (ranging up to 1870 ng mL^{-1}, (Li et al., 2018)). The range of PFOS to which humans are exposed differs between populations and both PFOS-02 and PFOS-53 can be considered human relevant concentrations. Furthermore, it is important to realize that the window of exposure in our study (22 h) was short compared to the *in vivo* situation where follicles grow for months. In addition, general populations are continuously exposed to complex mixture of compounds instead of single defined chemicals.

The most important route of exposure to humans is dietary intake primarily through drinking water and seafood (Poothong et al., 2020; Sunderland et al., 2019). Even though contamination of vegetables and plants does occur, it is not considered the main exposure (Ghisi et al., 2019). Hence, the background exposure of cattle (and the oocytes used in this study) is likely to be low under Swedish conditions. This is supported by a study in which PFOS concentrations in blood from cattle were considerably lower (on average 0.110 ng g^{-1}) compared to humans and the concentrations used in this experiment (Vestergren et al., 2013). In addition, the design of the experiments in this study counteracts any differences in exposure or physiology between individual cattle or herds of cattle by random distribution of oocytes between treated groups and control.

4.2. Altered embryo development after PFOS exposure

Following PFOS-02 exposure, there were no statistically significant negative effects on the proportion of embryos developing or on the quality or stage of the embryo using morphological assessments. However, after exposure to PFOS-53, we observed a decreased likelihood of cleaving to and beyond the two-cell stage 44 h after fertilisation. This suggests a direct effect of PFOS on the oocyte/cumulus cells that, in turn, affects the timing of the first cleavage divisions. Similarly, PFOS-53 embryos were delayed in the development into more advanced stages of blastocysts by day 8 (seen in PFOS-53 as both reduced stage and blastomere count). However, there was no reduction in the proportion of embryos developed compared to control, which indicate that the observed changes are more likely to be attributed to decreased developmental rate rather than early embryo lethality in this system.

Changed, and especially delayed development could have negative consequences for further development. Timing of events during early embryo development is important in bovines as well as in humans, and follows a strict and predictable timeline where deviations or delays are negative for further blastocyst development (Wong et al., 2010), and the timing of the first cleavage is predictive of blastocysts quality (Wang et al., 2014). Furthermore, the implantation window in humans is only about 48 h (Aghajanova et al., 2008). For successful implantation, the embryo and the endometrium must partake in a delicate communication where embryo as well as endometrial factors are of high importance (Diedrich et al., 2007) and delayed development might hamper this communication. Exposure to PFOS-53 was associated with inhibited *CTNNB1* signalling. This pathways seem to be important for blastocyst formation as *Ctnnb1* knockout mice embryos have abnormalities in shape and size (Messerschmidt et al., 2016). The exact role of *CTNNB1* in early embryo development is not fully understood but is linked to its involvement in *WNT*-signalling, which is crucial to a number of developmental processes (Tribulo et al., 2017). Furthermore, alteration of the *RELA* pathway after PFOS-53 exposure observed in this study might also play a role in the mechanisms of delayed/inhibited blastocyst formation. *RELA* is a subunit of the nuclear factor kappa B (*NF-κB*). *NF-κB* activation is required for the development of mouse embryos beyond the two-cell stage (Nishikimi et al., 1999). *NFKB1A* (inhibitor of *NF- κB*) transcript has been shown to decrease during oocyte IVM, but later increase as a

Table 2
Genes showing significant ($p < 0.05$) changes in both expression and DNA methylation in common pathways altered by PFOS-53.

Pathway	Gene Symbol	Expression	Methylation[a]	CpG Proximity[b]	Gene region[c]
TP53	ARPC1B	↑	↓	Shelf	Promoter
	ATP1A1	↑	↓	Open sea	Intron
	CARD10	↓	↑	Shelf	Promoter
	COL4A2	↑	↓	Island	Intron
	DDR1	↓	↓	Shelf	Promoter
	DKK3	↓	↓	Shore	Promoter/ Distal promoter
	DLC1	↑	↓	Shore	Intron
	EPAS1	↓	↑	Open Sea	Intron
	EPHA2	↓	↑	Shelf	Intron
	FASLG	↓	↓	Open Sea	Intron
	GPI	↑	↓	Open Sea	Intron
	HSPA1A/ HSPA1B	↑	↓	Island	Promoter
	HSPG2	↓	↓	Shore	Intron
	IGF1R	↑	↑	Open Sea	Intron
	IL2RA	↓	↑	Open Sea	Intron
	MTMR11	↓	↓	Open Sea	Promoter
	MYO1C	↑	↓	Island	Intron
	NAP1L4	↑	↓	Shore	Intron
	NOTCH1	↓	↓	Shelf	Intron
	PDE4B	↓	↓	Open Sea	Intron
	PDK2	↑	↑	Shelf	Promoter
	PMM1	↑	↓	Open Sea	Intron
	PPP1R13B	↑	↓	Shelf	Intron
	PRKAB1	↑	↑	Shelf	Intron
	PSAP	↑	↓	Island	Intron
	SCO1	↓	↑	Shore	Intron
	SEC23B	↑	↑	Island	Proximal promoter/ intron
	SLC6A6	↓	↑	Shore	Intron
	SNRK	↓	↓	Shore	Intron
	THY1	↑	↓	Shelf	Promoter/ Proximal promoter
	TMED7	↓	↓	Shelf	Intron
	ZAP70	↑	↑	Shelf	Intron
	ZFP36	↓	↓	Shelf	Exon/ Intron
TNF	ACACA	↑	↓	Shelf	Intron
	ADCY5	↓	↑	Open Sea	Intron
	ARSI	↓	↑	Shelf	Intron
	ATP1A1	↑	↓	Open Sea	Intron
	ATP2B4	↓	↑	Shelf	Intron
	CXCL2	↓	↓	Shelf	Promoter/ Proximal promoter
	EPHA2	↓	↑	Shelf	Intron
	FASLG	↓	↓	Open Sea	Exon/ Intron
	GOSR2	↑	↓	Open Sea	Intron
	HK3	↓	↓	Open Sea	Intron
	HSPA1A/ HSPA1B	↑	↓	Island	Promoter
	HSPG2	↓	↓	Shore	Intron
	IGF1R	↑	↑	Open Sea	Intron
	IL2RA	↓	↑	Open Sea	Intron
	ITPR1	↓	↑	Open Sea	Intron
	LRP6	↓	↓	Shelf	Promoter
	LTBR	↓	↓	Shelf	Proximal promoter
	MECP2	↓	↑	Shelf	Intron
	NGFR	↑	↓	Island	Proximal promoter
	NOTCH1	↓	↓	Shelf	Intron
	NR5A2	↓	↓	Shelf	Intron
	NSG1	↓	↓	Shelf	Intron
	PC	↑	↓	Open Sea	Intron
	PDE4B	↓	↓	Open Sea	Intron
	PTPRC	↓	↓	Shore	Intron
	SAMD4A	↑	↓	Open Sea	Intron
	SNRK	↓	↓	Shore	Intron
	ST3GAL5	↑	↑	Open Sea	Intron
	TBC1D8	↑	↑	Open Sea	Intron
	THY1	↑	↓	Shelf	Proximal promoter
	TWIST2	↓	↓	Shore	Promoter/ distal promoter
	ZFP36	↓	↓	Shelf	Intron/ Exon
CTNNB1	ACACA	↑	↓	Shelf	Intron
	BMP7	↓	↓	Shelf	Promoter/ proximal promoter
	COL4A2	↑	↓	Island	Intron
	CXCL2	↓	↓	Shelf	Promoter/ Proximal promoter
	EPHB4	↓	↑	Shelf	Promoter
	ERBB3	↑	↑	Shore	Intron
	FASLG	↓	↓	Open Sea	Intron
	IL2RA	↓	↑	Open Sea	Intron
	LRP6	↓	↓	Shelf	Promoter
	NGFR	↑	↓	Island	Proximal promoter
	NOTCH1	↓	↓	Shelf	Intron
	NR5A2	↓	↓	Shelf	Intron
	NUDT7	↓	↓	Open Sea	Intron
	PDE1C	↓	↓	Open Sea	Intron
	PDE4B	↓	↓	Open Sea	Intron
	PPP1R13B	↑	↓	Shelf	Intron
	PSAP	↑	↓	Island	Intron
	RASSF5	↑	↓	Shelf	Intron

[a] Arrow indicating hypermethylated (up) or hypomethylated (down) probe.
[b] CpG shore, shelves and open seas defined as located 1–2 kbp, 2–4 kbp or >4 kbp away from nearset CpG island.
[c] Proximal promoter, promoter and distal promoter region defined as first 1kbp, 5 kbp and 50 kbp of the transcriptomic start site.

consequence of embryo genome activation in the bovine model (Paciolla et al., 2011). There were further signs of impaired blastocyst formation and possibly also implantation by changed transcripts associated with *PTEN* signalling in blastocysts, which seem to be one of the important players for blastocyst formation and trophoblast invasion (Xue et al., 2020; Zhang et al., 2015). However, the process of implantation is complex and in many ways species-specific so to fully understand whether and how PFOS exposure during oocyte maturation could possibly affect the ability of embryos to implant, further experiments with an experimental set-up to investigate the effects on implantation are necessary.

During early development, mammalian embryos rely on pyruvate, fatty acids and amino acids as sources of energy. In bovines, the storage of lipids in droplets increases at morula-stage and decreases at blastocyst stage (Sudano et al., 2016) when the demand for lipids as an energy supply is high. Embryos respond to stress from environmental insults in different ways (see review by (Cagnone and Sirard, 2016)), and metabolic effects of stress include lipid accumulation (Abe et al., 2002; Romek et al., 2009). The increased lipid accumulation upon PFOS treatment observed in our study is supported by previous experiments in zebrafish embryos and larvae (Sant et al., 2021; Yi et al., 2019) and also in the amphibian *Daphnia magna* (Seyoum et al., 2020). The lipid accumulation after PFOS exposure in the livers of zebrafish fry has also been seen to be persistent after a period of recovery (Du et al., 2009) which stresses the fact that altered lipid metabolism in embryos might persist during further development. The altered lipid distribution during blastocyst stage is also consistent with findings from a previous study from our laboratory showing larger lipid droplets in bovine embryos

after exposure during IVM to sub-lethal concentrations of perfluorononanoic acid (PFNA) (Hallberg et al., 2019). Mechanisms underlying this altered lipid metabolism based on our molecular studies could involve *e.g.,* altered *NONO, APOE* and *JUN* pathways. Caveolin 1 (*CAV1*), which is a key player in the *JUN* pathway, plays an important role in lipid droplet maturation and biogenesis through cholesterol balance and lipid transport (Pol et al., 2001), and in lipid droplet size regulation in adipocytes (Blouin et al., 2010). It was recently shown that *CAV1* expression in bovine blastocysts is lower compared to porcine, and the difference was attributed to different lipid metabolisms between these species (Kajdasz et al., 2020). Furthermore, Acetyl-CoA carboxylase (ACC) coded by *ACACA* and was associated with *JUN* signalling upon PFOS exposure. This is the rate-limiting step in fatty acid synthesis and is increased in bovine embryos with higher oxidative stress and altered metabolism (Dos Santos et al., 2019). An increase in the other isoform of ACC, *acacab,* which mainly regulates fatty acid oxidation, and *acox1* gene expression has previously been demonstrated after developmental exposure of PFOS in zebrafish (Yi et al., 2019). The altered pathways in lipid metabolism imply that the surviving, morphologically normal embryos suppress lipid synthesis, possibly as an adaptive mechanism counteracting the PFOS induced lipid accumulation. The preimplantation embryo, although having limited capacity to respond to environmental insults, may alter transcriptome in order to survive (Puscheck et al., 2015).

PFOS has a known potential to activate the peroxisome-proliferator activated receptors (PPARs), (Behr et al., 2020; Khazaee et al., 2021; Shipley et al., 2004; Takacs and Abbott, 2007), which affect the lipid/glucose-metabolism, amongst other functions, leading to increased liver weight as a hallmark of PFOS toxicity in animal models. The mechanism of PFOS toxicity has been attributed partly, but not fully, to the activation of PPARα, and other nuclear receptors have also been shown to participate in PFOS response in both rat and human liver cells (Bjork et al., 2011). Apart from PPARα, PPARϒ and estrogen receptor-α (ERα) activation has been shown in mice (Rosen et al., 2017). Our results of delayed or possibly failed embryo development, as well as the lipid accumulation are similar to results in a study on mouse oocytes after exposure during IVM to a PPARϒ agonist (rosiglitazone, 20 μM). In that study, fatty acid oxidation was altered and, despite increasing the mitochondrial membrane potential, treatment was associated with impaired developmental competence and lower proportion of hatched blastocyst at day 5 (but no reduction in the proportion of blastocysts) (Dunning et al., 2014).

In both PFOS concentrations, pathways associated with apoptosis, cell proliferation and differentiation were altered showing clear signs of embryos coping with the previous insult of PFOS during IVM. This suggest that the decreased blastomere count and delayed developmental rate observed in PFOS-53 could be explained with increased apoptosis and/or decreased/delayed proliferation. This corresponds to previous studies of PFAS toxicity, where increased apoptosis during development has been demonstrated after PFOS exposure in *i.e.* zebrafish larvae (Shi et al., 2008) and *xenopus leavis* embryos (San-Segundo et al., 2016). *p53* signalling seems to be the key-player in apoptosis after both PFOA (Chen et al., 2017) and PFOS (Shi et al., 2008) exposure. In zebrafish, this PFOS induced apoptosis and *p53* activation has been attributed to ROS generation and *MAPK* signalling (Shi and Zhou, 2010). *P38 MAPK* is crucial for pre-implantation development, and inhibition has been associated with decreased expansion and hatching in the mouse (Bell and Watson, 2013), as well as increased apoptosis at blastocyst stage together with altered glucose metabolism (Sozen et al., 2015).

To interpret whether changes in gene expressions are more likely to be a transient adaptation to the surrounding environment or have more long-term effect on development, studies on the epigenome are necessary (Messerlian et al., 2017). The epigenome coordinates the responses that are adaptive in nature (Peters et al., 2021) and include histone tail modifications, chromatin remodelling and DNA methylation. DNA methylation is believed to have a major impact on gene silencing. Using a microarray platform developed for the bovine species (Montera et al., 2013), alterations in methylation patterns have been seen after exposure to altered metabolic situations (Laskowski et al., 2018) and environmental insults (Page-Lariviere et al., 2016). Following high DNA methylation during oocyte development (and during PFOS exposure), the epigenome, including the DNA methylome, is reprogrammed during the early stages of development in bovine and humans (Dean et al., 2003). During the period when the DNA methylation was studied (day eight of culture) the bovine genome starts to become remethylated after the active demethylation, and is at this point mostly related to the conservation of specific methylation sites from the parental chromosomes (Wang et al., 2014). During the following week of development, the embryo will continue the remethylation leading to a significantly higher methylation level on day twelve (Montera et al., 2013). The changes in methylation that we observe after exposure during the last stage of oocyte maturation are hence not only present a week later during development, but also conserved through DNA methylation erasure and reprogramming. The higher number of DMRs compared to DEGs can be explained by the fact that 1) the methylation microarray interrogates 10 times more probes compared to transcriptomic array (400,000 *vs* 40,000) and 2) methylation changes do not necessarily translate into changes in gene expression at this stage. We could observe similar biological functions altered as in the transcriptome profile related to cell death, apoptosis proliferation and differentiation. In fact, 59 of the genes in the in these pathways showed both transcriptional and DNA methylation changes upon PFOS-53 treatment. About half of these showed an inverse relationship between DNA methylation and gene expression change (18 of 33 TP53, 15 of 32 TNF and 8 of 18 CTNNB1) including promoter regions in CpG islands. This is line with the general suppressive function of DNA methylation. However, DNA methylation in gene bodies (Teissandier and Bourc'his, 2017) has been linked to increased gene transcription and even in promoter regions direct correlation between methylation and transcriptional activity can occur (Smith et al., 2020). Likewise, DNA methylation preventing transcriptional repressors to bind can lead to increased gene transcription (Ehrlich and Lacey, 2013). Such functions of DNA methylation might explain the cases where gene transcription and methylation was changed in the same direction by PFOS-53 exposure. Thus, this suggests that changes seen in the gene expression profile might be due to epigenetic alterations, and thus potentially persist during development. However, even though there is convincing evidence of developmental origin of later disease (Sinclair et al., 2007), the epigenetic mechanisms of gene programming during early embryo development are far from fully understood.

The phenotypic changes seen in the blastocysts upon PFOS exposure were modest and there were no evident embryo lethality at these exposure concentrations. This is likely reflected by the transcriptomic and the DNA methylation microarray results. Higher doses inducing larger morphological effects in the blastocyst would most likely have more impact with increased numbers of DEGs and DMRs. However, this would not reflect real-life exposures and thus not be within the scope of this study.

4.3. Implications for human health

PFOS exposure has been associated with decreased birth weight in humans, as well as an increased time to pregnancy (Fei et al., 2009; Whitworth et al., 2012). Decreased birth weight has also been demonstrated in rats (Luebker et al., 2005; Xia et al., 2011), although in combination with decreased weight gain in pregnant dams. Even though the processes are complex, delayed growth as early as the time for the first divisions of the zygote is predictive of later blastocyst quality in humans (Wang et al., 2014). Hence, the reduced growth during early embryo development resulting in inhibited or delayed blastocyst formation in day eight blastocyst might provide an insight to the mechanisms of the reduction in intrauterine growth and/or failed or impaired

implantation, resulting in reduced fecundity in humans.

There is evidence linking PFOS exposure to increased serum lipids and cholesterol in epidemiological studies, which is a risk factor for cardiovascular disease (Nelson et al., 2010; Steenland et al., 2009). Altered glucose and lipid metabolism has been seen in the adult offspring after exposure to PFOS *in utero* in experimental studies in mice (Lee et al., 2015; Wan et al., 2014), and PFOA has been suggested to have an obesogenic effect on offspring in human cohorts after exposure *in utero* (Halldorsson et al., 2012). The evidence for a causal association of *in utero* exposure to PFOS with metabolic effects such as diabetes and obesity is insufficient. However, our results of altered lipid metabolism during pre-implantation embryo development, together with previous *in vivo* studies showing disruption in fatty acid homeostasis in livers after oral exposure in rats (Curran et al., 2008) and altered glucose metabolism after *in utero* exposure in mice (Wan et al., 2014), provide further insight into PFOS toxicity influencing lipid metabolism of human relevance.

4.4. Conclusion

To conclude, we show that human relevant concentrations of PFOS alter early pre-implantation embryo development after short exposure during final oocyte maturation in a bovine model. Exposure to PFOS led to delayed development to more advanced blastocyst stages at concentrations of 53 ng mL^{-1} and transcriptomic alterations related to apoptosis, differentiation and proliferation, which was corroborated by epigenomic data one week after exposure. Similar effects were observed in the transcriptome and DNA methylation in blastocysts using 2 ng mL^{-1} exposure, suggesting that adverse effects might occur even at general population exposure levels. Effects on the epigenome suggest that if the embryo survives the PFOS insult, the effects may persist during further embryo and foetal development. This study emphasises the urgent need for remediation measures, adds to the evidence that PFOS exposure affects fertility and reproduction and may be useful for human health risk assessment.

Declaration of Competing Interest

The authors declare that they have no known competing financial interests or personal relationships that could have appeared to influence the work reported in this paper.

Acknowledgements

The authors acknowledge Dominic Gagné and Eric Fournier at EmbryoGENE for support during the laboratory work and bioinformatics. Petter Ranefall at BioImage Informatics Facility, Uppsala (funded by SciLifeLab, National Microscopy Infrastructure, NMI (VR-RFI 2019-00217) and the Chan-Zuckerberg Initiative) for providing expertise regarding image analysis. PFOS was kindly provided by Stefan Örn at SLU and Ida Crusell at SGS is acknowledged for validation of concentration in media. The authors also thank SCAN in Linköping for providing the ovaries for this work and Jonna Johansson for help in the IVF laboratory. This work was supported by FORMAS (Swedish Research Council for Environment, Agricultural Sciences and Spatial Planning, Grant No. 942-2015-476), Stiftelsen Nils Lagerlöfs fond (KSLA, GFS2017-0032) and Carl Tryggers stiftelse (CTS 17:413). Cells for Life Platform and Developmental Biology Platform at SLU for providing the facilities for this project, partly funded by the Infrastructure Committee, SLU, Sweden.

Appendix A. Supplementary data

Supplementary material related to this article can be found, in the online version, at doi:https://doi.org/10.1016/j.tox.2021.153028.

References

Abe, H., Yamashita, S., Satoh, T., Hoshi, H., 2002. Accumulation of cytoplasmic lipid droplets in bovine embryos and cryotolerance of embryos developed in different culture-system using serum-free or serum-containing media. Mol. Reprod. Dev. 61, 57–66.

Abraham, M.C., Gustafsson, H., Ruete, A., Brandt, Y., 2012. Breed influences on *in vitro* development of abattoir-derived bovine oocytes. Acta Veterinaria Scandinavia 54.

Aghajanova, L., Hamilton, A.E., Giudice, L.C., 2008. Uterine receptivity to human embryonic implantation: histology, biomarkers, and transcriptomics. Semin. Cell Dev. Biol. 19, 204–211.

Alm, H., Torner, H., Tiemann, U., Kanitz, W., 1998. Influence of organochlorine pesticides on maturation and postfertilization development of bovine oocytes in vitro. Reprod. Toxicol. 12, 559–563.

Barnes, F.L., First, N.L., 1991. Embryonic transcription in in vitro cultured bovine embryos. Mol. Reprod. Dev. 29, 117–123.

Behr, A.C., Plinsch, C., Braeuning, A., Buhrke, T., 2020. Activation of human nuclear receptors by perfluoroalkylated substances (PFAS). Toxicology In Vitro 62, 104700.

Bell, C.E., Watson, A.J., 2013. p38 MAPK regulates cavitation and tight junction function in the mouse blastocyst. PLoS One 8, e59528.

Bjerregaard-Olesen, C., Bach, C.C., Long, M., Ghisari, M., Bossi, R., Bech, B.H., Nohr, E. A., Henriksen, T.B., Olsen, J., Bonefeld-Jorgensen, E.C., 2016. Time trends of perfluorinated alkyl acids in serum from Danish pregnant women 2008-2013. Environ. Int. 91, 14–21.

Bjork, J.A., Butenhoff, J.L., Wallace, K.B., 2011. Multiplicity of nuclear receptor activation by PFOA and PFOS in primary human and rodent hepatocytes. Toxicology 288, 8–17.

Blazejczyk, M., Miron, M., Nadon, R., 2007. FlexArray: a Statistical Data Analysis Software for Gene Expression Microarrays. Genome Quebec, Montreal, Canada, 2007.

Blouin, C.M., Le Lay, S., Eberl, A., Kofeler, H.C., Guerrera, I.C., Klein, C., Le Liepvre, X., Lasnier, F., Bourron, O., Gautier, J.F., Ferre, P., Hajduch, E., Dugail, I., 2010. Lipid droplet analysis in caveolin-deficient adipocytes: alterations in surface phospholipid composition and maturation defects. J. Lipid Res. 51, 945–956.

Bombrun, M., Ranefall, P., Lindblad, J., Allalou, A., Partel, G., Solorzano, L., Qian, X., Nilsson, M., Wählby, C., 2017. Decoding gene expression in 2D and 3D. Image Analysis, pp. 257–268.

Cagnone, G., Sirard, M.A., 2016. The embryonic stress response to in vitro culture: insight from genomic analysis. Reproduction 152, R247–R261.

Calafat, A.M., Wong, L.-Y., Kuklenyik, Z., Reidy, J.A., Needham, L.L., 2007. Polyfluoroalkyl chemicals in the U.S. population: data from the national health and nutrition examination survey (NHANES) 2003–2004 and comparisons with NHANES 1999–2000. Environ. Health Perspect. 115, 1596–1602.

Chen, Y., Zhou, L., Xu, J., Zhang, L., Li, M., Xie, X., Xie, Y., Luo, D., Zhang, D., Yu, X., Yang, B., Kuang, H., 2017. Maternal exposure to perfluorooctanoic acid inhibits luteal function via oxidative stress and apoptosis in pregnant mice. Reprod. Toxicol. (Elmsford, N.Y.) 69, 159–166.

Curran, I., Hierlihy, S.L., Liston, V., Pantazopoulos, P., Nunnikhoven, A., Tittlemier, S., Barker, M., Trick, K., Bondy, G., 2008. Altered fatty acid homeostasis and related toxicologic sequelae in rats exposed to dietary potassium perfluorooctanesulfonate (PFOS). J. Toxicol. Environ. Health Part A 71, 1526–1541.

Dean, W., Santos, F., Reik, W., 2003. Epigenetic reprogramming in early mammalian development and following somatic nuclear transfer. Semin. Cell Dev. Biol. 14, 93–100.

DeLuca, N.M., Angrish, M., Wilkins, A., Thayer, K., Cohen Hubal, E.A., 2021. Human exposure pathways to poly- and perfluoroalkyl substances (PFAS) from indoor media: a systematic review protocol. Environ. Int. 146, 106308.

Diedrich, K., Fauser, B.C., Devroey, P., Griesinger, G., Evian Annual Reproduction Workshop, G, 2007. The role of the endometrium and embryo in human implantation. Hum. Reprod. Update 13, 365–377.

Ding, N., Harlow, S.D., Randolph Jr., J.F., Loch-Caruso, R., Park, S.K., 2020. Perfluoroalkyl and polyfluoroalkyl substances (PFAS) and their effects on the ovary. Hum. Reprod. Update 26, 724–752.

Dominguez, A., Salazar, Z., Arenas, E., Betancourt, M., Ducolomb, Y., Gonzalez-Marquez, H., Casas, E., Teteltitla, M., Bonilla, E., 2016. Effect of perfluorooctane sulfonate on viability, maturation and gap junctional intercellular communication of porcine oocytes in vitro. Toxicology In Vitro 35, 93–99.

Dos Santos, E.C., Varchetta, R., de Lima, C.B., Ispada, J., Martinho, H.S., Fontes, P.K., Nogueira, M.F.G., Gasparrini, B., Milazzotto, M.P., 2019. The effects of crocetin supplementation on the blastocyst outcome, transcriptomic and metabolic profile of in vitro produced bovine embryos. Theriogenology 123, 30–36.

Du, Y., Shi, X., Liu, C., Yu, K., Zhou, B., 2009. Chronic effects of water-borne PFOS exposure on growth, survival and hepatotoxicity in zebrafish: a partial life-cycle test. Chemosphere 74, 723–729.

Dunning, K.R., Anastasi, M.R., Zhang, V.J., Russell, D.L., Robker, R.L., 2014. Regulation of fatty acid oxidation in mouse cumulus-oocyte complexes during maturation and modulation by PPAR agonists. PLoS One 9, e87327.

Ehrlich, M., Lacey, M., 2013. DNA methylation and differentiation: silencing, upregulation and modulation of gene expression. Epigenomics 5, 553–568.

Fei, C., McLaughlin, J.K., Lipworth, L., Olsen, J., 2009. Maternal levels of perfluorinated chemicals and subfecundity. Hum. Reprod. 24, 1200–1205.

Feng, X., Wang, X., Cao, X., Xia, Y., Zhou, R., Chen, L., 2015. Chronic exposure of female mice to an environmental level of perfluorooctane sulfonate suppresses estrogen synthesis through reduced histone H3K14 acetylation of the StAR promoter leading to deficits in follicular development and ovulation. Toxicol. Sci. 148, 368–379.

Ghisi, R., Vamerali, T., Manzetti, S., 2019. Accumulation of perfluorinated alkyl substances (PFAS) in agricultural plants: a review. Environ. Res. 169, 326–341.
Gluge, J., Scheringer, M., Cousins, I.T., DeWitt, J.C., Goldenman, G., Herzke, D., Lohmann, R., Ng, C.A., Trier, X., Wang, Z., 2020. An overview of the uses of per- and polyfluoroalkyl substances (PFAS). Environ. Sci. Process. Impacts 22, 2345–2373.
Glynn, A., Berger, U., Bignert, A., Ullah, S., Aune, M., Lignell, S., Darnerud, P.O., 2012. Perfluorinated alkyl acids in blood serum from primiparous women in Sweden: serial sampling during pregnancy and nursing, and temporal trends 1996-2010. Environ. Sci. Technol. 46, 9071–9079.
Gonzalez, R., Sjunnesson, Y.C., 2013. Effect of blood plasma collected after adrenocorticotropic hormone administration during the preovulatory period in the sow on oocyte in vitro maturation. Theriogenology 80, 673–683.
Gordon, I., 1994. Laboratory Production of Cattle Embryos. Wallingford CAB International, Wallingford.
Gordon, I., 2003. Laboratory Production of Cattle Embryos. CABI Publishing, UK.
Grossman, D., Kalo, D., Gendelman, M., Roth, Z., 2012. Effect of di-(2-ethylhexyl) phthalate and mono-(2-ethylhexyl) phthalate on in vitro developmental competence of bovine oocytes. Cell Biol. Toxicol. 28, 383–396.
Gyllenhammar, I., Glynn, A., Benskin, J., Sandblom, O., Bignert, A., Lignell, S., 2017. Temporal Trends of Poly- and Perfluoroalkyl Substances (PFASs) in Pooled Serum Samples From First-Time Mothers in Uppsala, pp. 1997–2016.
Hallberg, I., Kjellgren, J., Persson, S., Orn, S., Sjunnesson, Y., 2019. Perfluorononanoic acid (PFNA) alters lipid accumulation in bovine blastocysts after oocyte exposure during in vitro maturation. Reprod. Toxicol. (Elmsford, N.Y.) 84, 1–8.
Halldorsson, T.I., Rytter, D., Haug, L.S., Bech, B.H., Danielsen, I., Becher, G., Henriksen, T.B., Olsen, S.F., 2012. Prenatal exposure to perfluorooctanoate and risk of overweight at 20 years of age: a prospective cohort study. Environ. Health Perspect. 120, 668–673.
Heffernan, A.L., Cunningham, T.K., Drage, D.S., Aylward, L.L., Thompson, K., Vijayasarathy, S., Mueller, J.F., Atkin, S.L., Sathyapalan, T., 2018. Perfluorinated alkyl acids in the serum and follicular fluid of UK women with and without polycystic ovarian syndrome undergoing fertility treatment and associations with hormonal and metabolic parameters. Int. J. Hyg. Environ. Health 221, 1068–1075.
IETS, 2010. Manual of the international embryo transfer society. In: Stringfellow, D.A., Givens, D.M. (Eds.), A Procedural Guide and General Information for the Use of Embryotransfer Technology Emphasizing Sanitary Procedures. International Embryo Transfer Society, 2441 Village Green Place, Champaign, Illinois 61822 USA.
Jorssen, E.P., Vergauwen, L., Goossens, K., Hagenaars, A., Van Poucke, M., Petro, E., Peelman, L., Knapen, D., Leroy, J.L., Bols, P.E., 2015. Optimisation of the bovine whole in vitro embryo system as a sentinel for toxicity screening: a cadmium challenge. Altern. Lab. Anim. 43, 89–100.
Kajdasz, A., Warzych, E., Derebecka, N., Madeja, Z.E., Lechniak, D., Wesoly, J., Pawlak, P., 2020. Lipid stores and lipid metabolism associated gene expression in porcine and bovine parthenogenetic embryos revealed by fluorescent staining and RNA-seq. Int. J. Mol. Sci. 21.
Kang, Q., Gao, F., Zhang, X., Wang, L., Liu, J., Fu, M., Zhang, S., Wan, Y., Shen, H., Hu, J., 2020. Nontargeted identification of per- and polyfluoroalkyl substances in human follicular fluid and their blood-follicle transfer. Environ. Int. 139, 105686.
Kannan, K., Corsolini, S., Falandysz, J., Fillmann, G., Kumar, K.S., Loganathan, B.G., Mohd, M.A., Olivero, J., Wouwe, N.V., Yang, J.H., Aldous, K.M., 2004. Perfluorooctanesulfonate and related fluorochemicals in human blood from several countries. Environ. Sci. Technol. 38, 4489–4495.
Kärrman, A., Ericson, I., van Bavel, B., Darnerud, P.O., Aune, M., Glynn, A., Lignell, S., Lindström, G., 2007. Exposure of perfluorinated chemicals through lactation: levels of matched human milk and serum and a temporal trend, 1996-2004, in Sweden. Environ. Health Perspect. 115, 226–230.
Khazaee, M., Christie, E., Cheng, W., Michalsen, M., Field, J., Ng, C., 2021. Perfluoroalkyl acid binding with peroxisome proliferator-activated receptors alpha, gamma, and delta, and fatty acid binding proteins by equilibrium dialysis with a comparison of methods. Toxics 9.
Kim, Y.R., White, N., Braunig, J., Vijayasarathy, S., Mueller, J.F., Knox, C.L., Harden, F. A., Pacella, R., Toms, L.L., 2020. Per- and poly-fluoroalkyl substances (PFASs) in follicular fluid from women experiencing infertility in Australia. Environ. Res. 190, 109963.
Krogenaes, A.K., Nafstad, I., Skåre, J.U., Farstad, W., Hafne, A., 1998. *In vitro* reproductive toxcicity of polychlorinated biphenyl congeners 153 and 126. Reprod. Toxicol. 12 (6), 575–580.
Laskowski, D., Sjunnesson, Y., Humblot, P., Sirard, M.A., Andersson, G., Gustafsson, H., Båge, R., 2016. Insulin exposure during in vitro bovine oocyte maturation changes blastocyst gene expression and developmental potential. Reprod. Fertil. Dev.
Laskowski, D., Båge, R., Humblot, P., Andersson, G., Sirard, M.A., Sjunnesson, Y., 2017. Insulin during in vitro oocyte maturation has an impact on development, mitochondria, and cytoskeleton in bovine day 8 blastocysts. Theriogenology 101, 15–25.
Laskowski, D., Humblot, P., Sirard, M.A., Sjunnesson, Y., Jhamat, N., Båge, R., Andersson, G., 2018. DNA methylation pattern of bovine blastocysts associated with hyperinsulinemia in vitro. Mol. Reprod. Dev. 85, 599–611.
Lee, Y.Y., Wong, C.K., Oger, C., Durand, T., Galano, J.M., Lee, J.C., 2015. Prenatal exposure to the contaminant perfluorooctane sulfonate elevates lipid peroxidation during mouse fetal development but not in the pregnant dam. Free Radic. Res. 49, 1015–1025.
Li, Y., Fletcher, T., Mucs, D., Scott, K., Lindh, C.H., Tallving, P., Jakobsson, K., 2018. Half-lives of PFOS, PFHxS and PFOA after end of exposure to contaminated drinking water. Occup. Environ. Med. 75, 46–51.
Lopez-Espinosa, M.J., Fletcher, T., Armstrong, B., Genser, B., Dhatariya, K., Mondal, D., Ducatman, A., Leonardi, G., 2011. Association of Perfluorooctanoic Acid (PFOA) and Perfluorooctane Sulfonate (PFOS) with age of puberty among children living near a chemical plant. Environ. Sci. Technol. 45, 8160–8166.
Luebker, D.J., Case, M.T., York, R.G., Moore, J.A., Hansen, K.J., Butenhoff, J.L., 2005. Two-generation reproduction and cross-foster studies of perfluorooctanesulfonate (PFOS) in rats. Toxicology 215, 126–148.
Mamsen, L.S., Jönsson, B.A.G., Lindh, C.H., Olesen, R.H., Larsen, A., Ernst, E., Kelsey, T. W., Andersen, C.Y., 2017. Concentration of perfluorinated compounds and cotinine in human foetal organs, placenta, and maternal plasma. Sci. Total Environ. 596-597, 97–105.
Mamsen, L.S., Bjorvang, R.D., Mucs, D., Vinnars, M.T., Papadogiannakis, N., Lindh, C.H., Andersen, C.Y., Damdimopoulou, P., 2019. Concentrations of perfluoroalkyl substances (PFASs) in human embryonic and fetal organs from first, second, and third trimester pregnancies. Environ. Int. 124, 482–492.
McCoy, J.A., Bangma, J.T., Reiner, J.L., Bowden, J.A., Schnorr, J., Slowey, M., O'Leary, T., Guillette Jr., L.J., Parrott, B.B., 2017. Associations between perfluorinated alkyl acids in blood and ovarian follicular fluid and ovarian function in women undergoing assisted reproductive treatment. Sci. Total Environ. 605–606, 9–17.
Ménézo, Y.J.R., Hérubel, F., 2002. Mouse and bovine models for human IVF*. Reprod. Biomed. Online 4, 170–175.
Messerlian, C., Martinez, R.M., Hauser, R., Baccarelli, A.A., 2017. 'Omics' and endocrine-disrupting chemicals — New paths forward. Nat. Rev. Endocrinol. 13, 740–748.
Messerschmidt, D., de Vries, W.N., Lorthongpanich, C., Balu, S., Solter, D., Knowles, B.B., 2016. Beta-catenin-mediated adhesion is required for successful preimplantation mouse embryo development. Development 143, 1993–1999.
Montera, Bd., Fournier, E., Saadi, H.A.S., Gagné, D., Laflamme, I., Blondin, P., Sirard, M.-A., Robert, C., 2013. Combined methylation mapping of 5mC and 5hmC during early embryonic stages in bovine. BMC Genomics 14.
Nelson, J.W., Hatch, E.E., Webster, T.F., 2010. Exposure to polyfluoroalkyl chemicals and cholesterol, body weight, and insulin resistance in the general U.S. population. Environ. Health Perspect. 118, 197–202.
Nishikimi, A., Mukai, J., Yamada, M., 1999. Nuclear translocation of nuclear factor kappa B in early 1-cell mouse Embryos1. Biol. Reprod. 60, 1536–1541.
Paciolla, M., Boni, R., Fusco, F., Pescatore, A., Poeta, L., Ursini, M.V., Lioi, M.B., Miano, M.G., 2011. Nuclear factor-kappa-B-inhibitor alpha (NFKBIA) is a developmental marker of NF-kappaB/p65 activation during in vitro oocyte maturation and early embryogenesis. Hum. Reprod. 26, 1191–1201.
Page-Lariviere, F., Tremblay, A., Campagna, C., Rodriguez, M.J., Sirard, M.A., 2016. Low concentrations of bromodichloromethane induce a toxicogenomic response in porcine embryos in vitro. Reprod. Toxicol. (Elmsford, N.Y.) 66, 44–55.
Page-Lariviere, F., Campagna, C., Sirard, M.A., 2017. Mechanisms involved in porcine early embryo survival following ethanol exposure. Toxicol. Sci. 156, 289–299.
Peters, A., Nawrot, T.S., Baccarelli, A.A., 2021. Hallmarks of environmental insults. Cell.
Petro, M.L.E., D'Hollander, W., Covaci, A., Bervoets, L., Fransen, E., De Neubourg, D., De Pauw, I., Leroy, J.L.M.R., Jorssen, E.P.A., Bols, P.E.J., 2014. Perfluoroalkyl acid contamination of follicular fluid and its consequence for *in vitro* oocyte developmental competence. Sci. Total Environ. 496, 282–288.
Pol, A., Luetterforst, R., Lindsay, M., Heino, S., Ikonen, E., Parton, R.G., 2001. A caveolin dominant negative mutant associates with lipid bodies and induces intracellular cholesterol imbalance. J. Cell Biol. 152, 1057–1070.
Poothong, S., Papadopoulou, E., Padilla-Sanchez, J.A., Thomsen, C., Haug, L.S., 2020. Multiple pathways of human exposure to poly- and perfluoroalkyl substances (PFASs): from external exposure to human blood. Environ. Int. 134, 105244.
Puscheck, E.E., Awonuga, A.O., Yang, Y., Jiang, Z., Rappolee, D.A., 2015. Molecular biology of the stress response in the early embryo and its stem cells. In: Leese, H.J., Brison, D.R. (Eds.), Cell Signaling During Mammalian Early Embryo Development. Springer, New York, New York, NY, pp. 77–128.
Ranefall, P., Sadanandan, S.K., Wählby, C., 2016. Fast adaptive local thresholding based on ellipse fit. 2016 IEEE 13th International Symposium on Biomedical Imaging (ISBI) 205–208.
Robert, C., Nieminen, J., Dufort, I., Gagne, D., Grant, J.R., Cagnone, G., Plourde, D., Nivet, A.L., Fournier, E., Paquet, E., Blazejczyk, M., Rigault, P., Juge, N., Sirard, M. A., 2011. Combining resources to obtain a comprehensive survey of the bovine embryo transcriptome through deep sequencing and microarrays. Mol. Reprod. Dev. 78, 651–664.
Romek, M., Gajda, B., Krzysztofowicz, E., Smorag, Z., 2009. Lipid content of non-cultured and cultured pig embryo. Reprod. Domest. Anim. 44, 24–32.
Rosen, M.B., Das, K.P., Rooney, J., Abbott, B., Lau, C., Corton, J.C., 2017. PPARalpha-independent transcriptional targets of perfluoroalkyl acids revealed by transcript profiling. Toxicology 387, 95–107.
Rotander, A., Kärrman, A., Toms, L.M., Kay, M., Mueller, J.F., Gomez Ramos, M.J., 2015. Novel fluorinated surfactants tentatively identified in firefighters using liquid chromatography quadrupole time-of-flight tandem mass spectrometry and a case-control approach. Environ. Sci. Technol. 49, 2434–2442.
Saadi, H.A.S., O'Doherty, A.M., Gagné, D., Fournier, É., Grant, J.R., Sirard, M.-A., Robert, C., 2014. An integrated platform for bovine DNA methylome analysis suitable for small samples. BMC Genomics 15.
San-Segundo, L., Guimaraes, L., Fernandez Torija, C., Beltran, E.M., Guilhermino, L., Pablos, M.V., 2016. Alterations in gene expression levels provide early indicators of chemical stress during Xenopus laevis embryo development: a case study with perfluorooctane sulfonate (PFOS). Ecotoxicol. Environ. Saf. 127, 51–60.
Sant, K.E., Annunziato, K., Conlin, S., Teicher, G., Chen, P., Venezia, O., Downes, G.B., Park, Y., Timme-Laragy, A.R., 2021. Developmental exposures to perfluorooctanesulfonic acid (PFOS) impact embryonic nutrition, pancreatic morphology, and adiposity in the zebrafish, Danio rerio. Environ. Pollut. 275, 116644.

Santos, R.R., Schoevers, E.J., Roelen, B.A., 2014. Usefulness of bovine and porcine IVM/IVF models for reproductive toxicology. Reprod. Biol. Endocrinol. 12.
Schrenk, D., Bignami, M., Bodin, L., Chipman, J.K., Del Mazo, J., Grasl-Kraupp, B., Hogstrand, C., Hoogenboom, L.R., Leblanc, J.C., Nebbia, C.S., Nielsen, E., Ntzani, E., Petersen, A., Sand, S., Vleminckx, C., Wallace, H., Barregard, L., Ceccatelli, S., Cravedi, J.P., Halldorsson, T.I., Haug, L.S., Johansson, N., Knutsen, H.K., Rose, M., Roudot, A.C., Van Loveren, H., Vollmer, G., Mackay, K., Riolo, F., Schwerdtle, T., 2020. Risk to human health related to the presence of perfluoroalkyl substances in food. EFSA J. 18, e06223.
Seyoum, A., Pradhan, A., Jass, J., Olsson, P.E., 2020. Perfluorinated alkyl substances impede growth, reproduction, lipid metabolism and lifespan in Daphnia magna. Sci. Total Environ. 737, 139682.
Shi, X., Du, Y., Lam, P.K., Wu, R.S., Zhou, B., 2008. Developmental toxicity and alteration of gene expression in zebrafish embryos exposed to PFOS. Toxicol. Appl. Pharmacol. 230, 23–32.
Shi, X., Zhou, B., 2010. The role of Nrf2 and MAPK pathways in PFOS-induced oxidative stress in zebrafish embryos. Toxicol. Sci. 115, 391–400.
Shipley, J.M., Hurst, C.H., Tanaka, S.S., DeRoos, F.L., Butenhoff, J.L., Seacat, A.M., Waxman, D.J., 2004. Trans-activation of PPARalpha and induction of PPARalpha target genes by perfluorooctane-based chemicals. Toxicol. Sci. 80, 151–160.
Sinclair, K.D., Lea, R.G., Rees, W.D., Young, L.E., 2007. The developmental origins of health and disease: current theories and epigenetic mechanisms. Soc. Reprod. Fertil. Suppl. 64, 425–443.
Smith, J., Sen, S., Weeks, R.J., Eccles, M.R., Chatterjee, A., 2020. Promoter DNA hypermethylation and paradoxical gene activation. Trends Cancer 6, 392–406.
Sozen, B., Ozturk, S., Yaba, A., Demir, N., 2015. The p38 MAPK signalling pathway is required for glucose metabolism, lineage specification and embryo survival during mouse preimplantation development. Mech. Dev. 138 (Pt 3), 375–398.
Steenland, K., Tinker, S., Frisbee, S., Ducatman, A., Vaccarino, V., 2009. Association of perfluorooctanoic acid and perfluorooctane sulfonate with serum lipids among adults living near a chemical plant. Am. J. Epidemiol. 170, 1268–1278.
Sudano, M.J., Rascado, T.D., Tata, A., Belaz, K.R., Santos, V.G., Valente, R.S., Mesquita, F.S., Ferreira, C.R., Araujo, J.P., Eberlin, M.N., Landim-Alvarenga, F.D., 2016. Lipidome signatures in early bovine embryo development. Theriogenology 86 (472-484), e471.
Sunderland, E.M., Hu, X.C., Dassuncao, C., Tokranov, A.K., Wagner, C.C., Allen, J.G., 2019. A review of the pathways of human exposure to poly- and perfluoroalkyl substances (PFASs) and present understanding of health effects. J. Expo. Sci. Environ. Epidemiol. 29, 131–147.
Takacs, M.L., Abbott, B.D., 2007. Activation of mouse and human peroxisome proliferator-activated receptors (alpha, beta/delta, gamma) by perfluorooctanoic acid and perfluorooctane sulfonate. Toxicol. Sci. 95, 108–117.
Teissandier, A., Bourc'his, D., 2017. Gene body DNA methylation conspires with H3K36me3 to preclude aberrant transcription. EMBO J. 36, 1471–1473.
Tribulo, P., Moss, J.I., Ozawa, M., Jiang, Z., Tian, X.C., Hansen, P.J., 2017. WNT regulation of embryonic development likely involves pathways independent of nuclear CTNNB1. Reproduction 153, 405–419.
UNEP, 2009. All POPs Listed in the Stockholm Convention.
Velez, M.P., Arbuckle, T.E., Fraser, W.D., 2015. Maternal exposure to perfluorinated chemicals and reduced fecundity: the MIREC study. Hum. Reprod. 30, 701–709.
Vestergren, R., Orata, F., Berger, U., Cousins, I.T., 2013. Bioaccumulation of perfluoroalkyl acids in dairy cows in a naturally contaminated environment. Environ. Sci. Pollut. Res. Int. 20, 7959–7969.
Wan, H.T., Zhao, Y.G., Leung, P.Y., Wong, C.K., 2014. Perinatal exposure to perfluorooctane sulfonate affects glucose metabolism in adult offspring. PLoS One 9, e87137.
Wang, L., Zhang, J., Duan, J., Gao, X., Zhu, W., Lu, X., Yang, L., Zhang, J., Li, G., Ci, W., Li, W., Zhou, Q., Aluru, N., Tang, F., He, C., Huang, X., Liu, J., 2014. Programming and inheritance of parental DNA methylomes in mammals. Cell 157, 979–991.
Whitworth, K.W., Haug, L.S., Baird, D.D., Becher, G., Hoppin, J.A., Skjaerven, R., Thomsen, C., Eggesbo, M., Travlos, G., Wilson, R., Longnecker, M.P., 2012. Perfluorinated compounds and subfecundity in pregnant women. Epidemiology 23, 257–263.
Wikström, S., Lin, P.I., Lindh, C.H., Shu, H., Bornehag, C.G., 2020. Maternal serum levels of perfluoroalkyl substances in early pregnancy and offspring birth weight. Pediatr. Res. 87, 1093–1099.
Wong, C.C., Loewke, K.E., Bossert, N.L., Behr, B., De Jonge, C.J., Baer, T.M., Reijo Pera, R.A., 2010. Non-invasive imaging of human embryos before embryonic genome activation predicts development to the blastocyst stage. Nat. Biotechnol. 28, 1115–1121.
Xia, W., Wan, Y., Li, Y.Y., Zeng, H., Lv, Z., Li, G., Wei, Z., Xu, S.Q., 2011. PFOS prenatal exposure induce mitochondrial injury and gene expression change in hearts of weaned SD rats. Toxicology 282, 23–29.
Xue, P., Fan, W., Diao, Z., Li, Y., Kong, C., Dai, X., Peng, Y., Chen, L., Wang, H., Hu, Y., Hu, Z., 2020. Up-regulation of PTEN via LPS/AP-1/NF-kappaB pathway inhibits trophoblast invasion contributing to preeclampsia. Mol. Immunol. 118, 182–190.
Yi, S., Chen, P., Yang, L., Zhu, L., 2019. Probing the hepatotoxicity mechanisms of novel chlorinated polyfluoroalkyl sulfonates to zebrafish larvae: implication of structural specificity. Environ. Int. 133, 105262.
Zhang, Y., Beesoon, S., Zhu, L., Martin, J.W., 2013. Biomonitoring of perfluoroalkyl acids in human urine and estimates of biological half-life. Environ. Sci. Technol. 47, 10619–10627.
Zhang, C., Shi, Y.R., Liu, X.R., Cao, Y.C., Zhen, D., Jia, Z.Y., Jiang, J.Q., Tian, J.H., Gao, J. M., 2015. The anti-apoptotic role of Berberine in preimplantation embryo in vitro development through regulation of miRNA-21. PLoS One 10, e0129527.
Zhou, W., Zhang, L., Tong, C., Fang, F., Zhao, S., Tian, Y., Tao, Y., Zhang, J., Shanghai Birth Cohort, S, 2017. Plasma perfluoroalkyl and polyfluoroalkyl substances concentration and menstrual cycle characteristics in preconception women. Environ. Health Perspect. 125, 067012.